

We thank the reviewers for the helpful comments! We have now taken the benefit from those in improving the manuscript. A point by point response by a reply or/and actions (in black) to the reviewers' comments (in blue) will follow. New texts added or removed are shown in italics. The aim was to reply on each comment separately even if it creates some repetitions in replies (several comments solved by similar change). However, due to the number of comments there are a few that become obsolete due to changes from others. Then that are described by a reply. At the end is the full manuscript with changes in "track changes mode".

## Response to Anonymous Referee #1

This manuscript describes data collected from a FIGAERO-CIMS during laboratory studies using the flow reactor GFROST. Focus is given on the major organic nitrate constituents of secondary organic aerosol from the NO<sub>3</sub> oxidation of limonene. A cluster-analysis method is used in order to distinguish the groups of ions based on their thermodynamic properties and molecular formula information. Mechanisms of dimer formation are suggested based on the grouping performed. The paper is suitable for publication in ACP. My suggestions below are mainly to clarify the presentation

**Reply:** Thanks for the suggestions to clarify the presentation.

Specific comments 1. Recent studies have shown that fragmentation due to thermal dissociation in the FIGAERO-CIMS could strongly affect the chemical formula attribution (Stark et al., 2017). It would be beneficial if a comparison of the different methods of assigning a chemical formula to the major ions could be performed. If not, then the possible uncertainties introduced should be further discussed.

**Reply:** Yes, we should more clearly acknowledge the possibilities for decomposition but would rather be brief and refer to the findings in the Stark et al paper.

**Action:** Reference added with short notice on fragmentation.

*"Recently, Stark et al. (2017) showed that fragmentation during the desorption can occur within the FIGAERO. In the current work the fragmentation within the FIGARO was not specifically investigated. However, from our cluster analysis it was evidently that fragmentation occurred with specific features in e.g. molecular weight and evaporation temperature. The ramp rate during desorption was therefore maintained for all experiments to ensure, if fragmentation did occur, it would be consistent and enable comparable analysis of the dataset"*

2. In line 98 it is mentioned that one of the main focuses of this paper is to determine the molecular formula of species that could contribute significantly to SOA formation. Although the uncertainty of calculating the mass concentration using FIGAERO-CIMS would be high it could still indicate whether the compounds measured are indeed a large fraction of the overall mass as has been done from Isaacman-VanWertz et al. (2017).

**Reply:** Assuming common sensitivities for all compounds would enable the reader to find the major contributors to SOA mass in the list of compounds (Table S1 supplemental). The application of various sensitivities for I-CIMS is to date very uncertain and discussed in the literature, e.g. Isaacman-VanWertz et al. (2017).

**Action:** The Isaacman-VanWertz et al. (2017) has been added as reference for current state where they summarising methods to derive concentrations from I-CIMS . In addition, a short notice on the issue brought up by the referee with reference to Table 1 has been added.

*“This list is based on a common sensitivity for detection that might not always be true and highly variable (see e.g. Isaacman-Van Wertz et al, 2017). However, with this assumption the list will provide molecular identity of the most prominent organic compounds contributing to the SOA mass outlined in Table 1. One could assess the contribution of these peaks to the total mass loading, although with high variation in molecular mass and oxidation, the sensitivity is likely to vary significantly, resulting in large error margins and therefore deeming any interpretation highly speculative.”*

3. FIGAERO-CIMS collects both the gas and particle phase compounds on the filter. More information on the gas phase compounds detected would bring light concerning the extent of possible gas phase “interference” during desorption. When the signal of the compounds in the gas phase is high then their contribution to the aerosol during desorption could increase more. Have there been any checks on the contribution of gas phase signal during desorption? How much is it expected to be in the monomer and how much in the dimer range? A figure to illustrate this effect in the supplementary would be very informative. For example, in lines 346-348 this could also be due to gas phase compounds collected on the filter that undergo evaporation and thus contribute to the aerosol. What is the gas phase concentration of these compounds compared to the aerosol?

**Reply:** The methods and potential artifacts have been described in previous publications. Generally, there are limiting gas-phase contaminations of the condensed phase evaporation. Yes, the gas-phase has also been measured and could be presented to illustrate the ratio between gas and particle phase concentrations.

**Action:** Two figures illustrating partition (ratio between the particle and the gas phase) for ions in monomer and dimer region has been added in supplemental (Fig S1). A note at the end of first paragraph in section 3.1 now reads:

*“The gas to particle ratio of most ions were below one as illustrated in Fig. S1, whereas the focus of this work was to characterize the particle phase.”*

4. In Figure 3 for many of the compounds there is a residual signal above zero. How would that affect the signal of the next desorption? When FIGAERO reaches stable conditions what does that exactly mean? It would be fruitful for the reader if background measurements could be provided during these experiments on the Supplementary material. An additional figure to support the stability of the thermograms would be very instructive. For example the average cumulative signal (with error bars indicating the standard deviation of the average) vs temperature, for each compound, with each compound indicated with a different color would be a suggested way.

**Reply:** Usually several cycles are repeated and an average of three desorptions are used for the results

**Action:** Examples of three consecutive desorptions are now presented in supplemental (see Fig S2). The text refers to this figure in the experimental part. It now reads:

*“An average of four sequential desorption with corresponding standard deviation is shown in Fig. S2.”*

5. What is the atmospheric relevance with the mixing ratio of N<sub>2</sub>O<sub>5</sub> used? What is the NO<sub>3</sub> expected mixing ratio in the system? A discussion would better inform the reader.

**Reply:** Obviously, the mixing ratio of N<sub>2</sub>O<sub>5</sub> is higher than ambient to provide enough amount of limonene reacting during the time spent in the flow reactor. At a ratio of 1:1 we expect NO<sub>3</sub> to primarily react with the exocyclic double bond, representing the typical case producing primary products, while increasing the ratio will add more possibilities for reactions also to the endocyclic double bond reflecting secondary atmospheric chemistry.

**Action:** Short discussion on our view on this has been added in the in experimental:

*“At a ratio around 1.0 one expects only the endocyclic double bond to be reacting with NO<sub>3</sub> radicals while at higher ratio there is an increased possibility for secondary chemistry where products will be susceptible for reaction with the NO<sub>3</sub> radical.”*

6. In Figure 4 what is the fit function used? What is the information we gain from this fit choice? Further discussion in the manuscript would clarify these questions. This figure doesn't provide all the data points seen in Table 1. The high N<sub>2</sub>O<sub>5</sub>/limonene ratio of 113.3 is missing. Could that be included or provided in the supplementary? Is this point included in the fit function applied now? Finally, error bars for the y-axis are missing and the fit function should be applied by taking into account this error.

**Reply:** yes, we agree the line is mostly for guidance of the eye and the r<sup>2</sup> should be removed. The data point at 113.3 was not illustrated as it would extend the x-axes too far.

**Action:** The r<sup>2</sup> has been removed and the missing data point at 113 and its corresponding values are now noted in the footnote. The end of the Figure caption now reads:

*“The data points at a ratio of 113 are not shown (22, 78, 39%, respectively). The lines indicated are for the guidance of the eye.”*

7. In section 2.3 was it both gas and particle phase data used as identified species to compare to the MCM? A sentence to make clear that this work is focused on the particulate phase and not the gas phase would better direct the reader at this point.

**Reply:** The HR fitting procedure used ions both from gas and particle phase.

**Action:** A note has been added to direct the reader on this point at the end of the sentence:

*“...the corresponding theoretical product distribution was compared with the measured distribution for both gas and particle phase.”*

To further stress the focus on condensed phase a sentence was added in first part of R&D.

*“The focus in the current work was on condensed phase products using the FIGARO inlet desorption”*

8. It would be beneficial for the reader if the discussion in section 3.4 was extended on how the suggested mechanisms can be directly inferred from the grouping technique and the volatility of the compounds.

**Reply:** The lower O/C ratios and loss of one nitrogen compound for some of the dimers while exhibiting a low volatility would support the mechanism suggested. (loss of oxygen(s) and nitrogen in dimerisation)

**Action:** This info has now been rewritten and the initial text now reads:

*“The mechanism to create dimers with one nitrogen and a lower O/C ratio would presumably involve the loss of a nitrogen oxides or nitric acid. For this complex system and within the scope of this study it was not possible to firmly proof any mechanism. Since the experiment were done at low RH the direct hydrolysis would be less likely (see Rindelaub et al, 2015, 2016). However, knowing HNO<sub>3</sub> being thermodynamic stable one may speculate in that dimerization of two monomer species via the loss of one HNO<sub>3</sub> molecule could occur e.g. where a C<sub>20</sub>H<sub>29</sub>NO<sub>y</sub> (y = 10–18) species would be generated from C<sub>10</sub>H<sub>15</sub>NO<sub>x</sub> (x = 5–9) species. This process could be seen as the reverse of esterification in order to produce a dimer product with one less nitrogen and reduced numbers of oxygens.”*

#### Technical comments

Line 47. A broader view of organic nitrates is given by Kiendler-Scharr (2016).

**Action:** Reference added

Line 154. Units are missing.

**Action:** Units of g cm<sup>-3</sup> have been added

Line 167. Delete one dot.

**Action:** Full stop deleted

Line 234. Recent findings suggest that fragmentation due to thermal dissociation occurs in systems like the FIGAERO-CIMS (Stark et al., 2017). See comment 1.

**Action:** The following text has been added to acknowledge the work of Stark *et al.* (2017) and we have considered for possibilities that ions may fragment upon desorption:

*“Recently, Stark et al. (2017) showed that fragmentation during the desorption can occur within the FIGAERO. In the current work the fragmentation within the FIGARO was not specifically investigated. However, from our cluster analysis it was evidently that fragmentation occurred with specific features in e.g. molecular weight and evaporation temperature. The ramp rate during desorption was therefore maintained for all experiments to ensure, if fragmentation did occur, it would be consistent and enable comparable analysis of the dataset”*

Line 324-337. The authors provide four characteristic desorption patterns and the numbering stops at two.

**Action:** Addition numbering has been added in the text.

Line 361-362. It would be more informative to add the positive correlation in the supplement as a figure.

**Action:** The text refers to Fig. 5a. However, it has now been moved and clarified (since the trend is only valid for part of the data and Fig5a is discussed later in the text). It now reads:

*“A positive trend between the MW and  $T_{max}$  values, see Fig 5a., was obtained for data in two of the monomer clusters (1 and 2) and the high volatile dimer cluster, while the trend turned negative for the low volatile dimers cluster.”*

Line 387. Please define what extremely low signal would be as a value.

**Action:** A definition has now been added.

*“extremely low signal (i.e. the thermogram did not exhibit any structure identifiable above background noise prohibiting Tofware to constrain a mathematical fit for Tmax calculations)”*

Line 428. Should be 0-2?

**Action:** Changed to 0-2 in text

Table 1. Sorting of the lists would make the table more readable. Sorting the N2O5 from low to high and within each N2O5 group sorting the limonene from low to high would be one way of performing the sorting. Adding the expected NO3 concentration would be fruitful. Errors for the average SOA mass measured from an SMPS are missing. An additional column of the mass FIGAERO-CIMS could detect (with its much higher uncertainty), as discussed above, would be an indicator of how much of the overall SOA mass is measured in this system.

**Action:** The Table has been ordered as suggested by the reviewer. We did not measure the actual NO<sub>3</sub> concentrations and the total mass from FIGAERO-CIMS is rather uncertain. However, the standard deviation of the mean SOA mass is now included in the Table.

Table 2. What is the information we gain from the (N/C)x10? Based on all uncertainties the temperature precision could be rounded. Error of the average contribution is missing.

**Action:** The column displaying N/Cx10 has been removed. The temperatures have been rounded to the nearest degree. Errors of the average contributions are now included.

Figure 3. Certain double peak compounds are not highlighted like C10H15NO7, C20H29NO5, C20H24N2O8 etc. The C20H24N2O8 is not written correctly in the annotation. Since there are more compounds that have double peaks plotted it would be clearer to include the double peak compounds with dash lines and avoid highlighting.

**Action:** The highlighting has been removed and the mis-formatted compound name (C<sub>20</sub>H<sub>24</sub>N<sub>2</sub>O<sub>8</sub>) has been corrected.

Figure 5. It improves the figure if (a) and (b) have the same annotation introduced on the right side outside both figures once. This way you avoid the change in font size that is seen for annotation from Figure (a). For Figure (b) the oxidation state is not mentioned in the axis and the range is not going to minus when it is below zero. It would be beneficial if Figure (c) was separated in two graphs. On the left side a figure of the MW (left-axis) and Tmax (right-axis) and on the right side a figure of the oxidation state (left-axis) and the O/C (right-axis). Box-and-whiskers instead of bars and markers would provide more information on the dataset. This would also show more clearly the temperature increase that is suggested to correlate to the O/C increase. Finally the colors of Figure (c) are similar to the colors of the clusters thus confusing the reader.

**Action:** Changed the plot to a 4-panel plot by separating the bottom graph. The other minor formatting issues were also fixed, like the single legend for the top plots.

References Isaacman-VanWertz, G., P. Massoli, R. E. O'Brien, J. B. Nowak, M. R. Canagaratna, J. T. Jayne, D. R. Worsnop, L. Su, D. A. Knopf, P. K. Misztal, C. Arata, A. H. Goldstein, and J. H. Kroll: Using advanced mass spectrometry techniques to fully characterize atmospheric organic carbon: current capabilities and remaining gaps, *Faraday Discussions*, doi:10.1039/C7FD00021A, 2017.

Kiendler-Scharr, A.: Ubiquity of organic nitrates from nighttime chemistry in the European submicron aerosol, *Geophys. Res. Lett.*, 43, 7735–7744, doi:10.1002/, 2016.

Stark, H., R. L. N. Yatavelli, S. L. Thompson, H. Kang, J. E. Krechmer, J. R. Kimmel, B. B. Palm, W. Hu, P. L. Hayes, D. A. Day, P. Campuzano-Jost, M. R. Canagaratna, J. T. Jayne, D. R. Worsnop, and J. L. Jimenez: c, *Environ Sci Technol*, doi:10.1021/acs.est.7b00160, 2017.

## Response to Anonymous Referee #2

General comments: This paper presents novel flow tube measurements of the chemical composition of SOA produced from  $\text{NO}_3$  + limonene, with the potential to provide valuable new mechanistic clues and making the (as far as I know) new proposal that dimer formation reactions may be accompanied by  $\text{HNO}_3$  loss, as a possible explanation for the C20 compounds observed with only a single N. The authors also describe observed thermal desorption profiles that hint at monomers coming from dimer dissociation in the instrument inlet, an important caution to other researchers using this technique. For these reasons, I think this manuscript will be a valuable contribution to the atmospheric chemistry literature, but it needs substantially more work before it is ready for publication. First, in many places I found the writing confusing and had a difficult time understanding what the authors were saying – I think this draft was at least one round of serious editing away from being ready to submit. I'll flag the sentences I found most confusing below, but after edits, I urge the authors to also find another outside reader to go through the entire manuscript. Second, and more importantly, the analysis of this rich dataset feels incomplete. At present, the paper really just presents FIGAERO MS and thermogram results, cluster analysis, and the  $\text{HNO}_3$  loss mechanism idea, without much support beyond the chemical formulae observed. I make the following broad suggestions for the authors to further this analysis before resubmitting for publication:

**Reply:** Actually, the manuscript had been sent for English language editing service. However, we might have missed that some of the changes suggested by the English language editing back-fired on the scientific clarity before submission. The paper has now been read again and we have addressed the issues raised by the three referees which make the science more clear.

(1) present a better foundation for the idea of  $\text{HNO}_3$  loss: show a proposed structural mechanism for how this would occur, cite additional literature on the energetics of such a reaction and of any other experiments that made observations consistent with this proposal, and try to produce an (even coarse) nitrogen budget from your experiments to check if it supports  $\text{HNO}_3$  loss. How much of the  $\text{N}_2\text{O}_5$  you injected didn't show up in gas or aerosol phase CIMS products? is any change in this budget over different experiments consistent with the amount of the products you hypothesize to come from this type of reaction?

**Reply:** There are some suggestions in the literature, however, it is not as clear as one hope it should be and we cannot firmly conclude this so we have to leave that open for speculations and following up-studies on simpler systems. The nitrogen budget would be useful but since  $\text{HNO}_3$  is notorious to be "sticky" and we did not measure the other suspected "leaving groups" like  $\text{NO}_2$  and  $\text{NO}$  we have poor handled on this. However, it is clear that the selected dimers only contain one nitrogen and have lower O/C ratio than the sum of two monomers. Furthermore, the  $T_{\text{max}}$  suggests a high Mw compound (with low vapor pressure) and not a fragment.

**Action:** We now refer to some recent literature on organic nitrate condensed phase reactions (hydrolysis) and clarify our speculation further.

*"The mechanism to create dimers with one nitrogen and a lower O/C ratio would presumably involve the loss of a nitrogen oxides or nitric acid. For this complex system and within the scope of this study it was not possible to firmly proof any mechanism. Since the experiment were done at low RH the direct hydrolysis would be less likely (see Rindelaub et al, 2015, 2016). However, knowing  $\text{HNO}_3$  being*

*thermodynamic stable one may speculate in that dimerization of two monomer species via the loss of one HNO<sub>3</sub> molecule could occur e.g. where a C<sub>20</sub>H<sub>29</sub>NO<sub>y</sub> (y = 10–18) species would be generated from C<sub>10</sub>H<sub>15</sub>NO<sub>x</sub> (x = 5–9) species. This process could be seen as the reverse of esterification in order to produce a dimer product with one less nitrogen and reduced numbers of oxygens.”*

(2) The cluster analysis should also be analyzed and discussed in greater detail: thus far, it seems to serve only to highlight the same two “groups” as the MS alone would have – the monomer region (in 3 factors) and the dimer region (in 2 factors). You mention the families in each cluster and have generic chemical formulae for them. Can you propose structures / reasons these would be different? Are they potentially from oxidation at the different double bonds (what would you expect that to look like?) or form RO<sub>2</sub> + RO<sub>2</sub> reactions vs. RO<sub>2</sub> + NO<sub>3</sub> reactions? Why is cluster 0 basically spread across the O/C and MW space of clusters 1 and 2 – why is it nevertheless a separate cluster? Is there any proposed mechanism that would get you this, or could it be that cluster 0 are the fragments of dimers while 1 and 2 are straight monomers? Or, some permutation of this?

**Reply:** Maybe, this was the information that was not so clear. However, it is actually stated that cluster 0 is not similar to the monomer cluster 1 and 2 but rather a fragmentation cluster having similar Mw and O/C but different Tmax (much higher). The reason for family m5 and m7 residing exclusively in factor 1 (higher volatility) is not known but clearly interesting results. Generally, its obviously good that the cluster analysis confirm the more commonly “by the eye” definition on monomer and dimer regions from inspection of the mass spectra alone.

**Action:** The discussions and the actual Fig. 5 has been changed according to a number of other comments.

(3) It seems you should also be able to do more with the fact that some monomers have double peaks and some don't – can you correlate this to the cluster analysis somehow, or otherwise interpret it mechanistically?

**Reply:** Yes, this is already included in the analysis. Some ions has two desorption maximum and then T<sub>max,2</sub> was also added in the analysis. E.g. cluster 0 contains mainly ions with a T<sub>max,2</sub>

(4) You mention that some observed formulae are in MCM and others are not. Do more with this. Are there any structures predicted to be major products in MCM that you don't observe? I would suggest to show a modeled output of MCM (just a box model) for your expt. conditions. Are the major few predicted products all those that you observe, or are you just observing one product channel / some at random / etc.? You have the data now to truly test the MCM (and you allude to it), and I was disappointed to see that you didn't report a true comparison. For the major formulae that you observed that aren't in MCM, too, I'd like to see more analysis. You say in your conclusions that these should be included in models, but you haven't told us what they might be. Propose some structures / mechanistic origins / something based on MCM to help guide how your novel observations might be incorporated.



**Reply:** As stated in the paper 69% of the gas-phase compounds could be referred to MCM compounds (assuming a common sensitivity). Yes, we should have presented an output from MCM model to compare with observed condensed phase products.

**Action:** The MCM run provided a list of major compounds that is now presented in the supplemental information (Table S1).

(5) Suggest to read this recent NO<sub>3</sub> + limonene paper from the Ng group: <http://pubs.acs.org/doi/abs/10.1021/acs.est.7b01460> and include comparisons to these results in your updated draft. Can you make any quantitative estimate of SOA yields to compare to Boyd et al.'s (very high!!) SOA yields from NO<sub>3</sub> + limonene, or comment on them based on your mechanism? Are >100% yields consistent with your proposed dimerization mechanism, or inconsistent? Please discuss.

**Reply:** We realized that this is a recent study that was done in parallel to our work. However, if not necessary we prefer not to explicitly present aerosol yields from a flow reactor study. Furthermore, with a very different method we abstain also from comments on their high yield. The dimerization mechanism would if anything enhance an aerosol yield since it will increase the observed T<sub>max</sub>.

#### Specific editorial suggestions:

in title: "nitrate-radical-initiated" should be "nitrate radical-initiated", and elsewhere in text

**Action:** This has been changed accordingly.

line 11 "reaction of NO<sub>3</sub> with limonene"

**Action:** Text changed to recommended text (replace "and" to "with")

line 14 "identity and volatility of the most" Sentence line 17-19 is confusing. How about: "The observed products were compared to those in the Master Chemical Mechanism (MCM) limonene mechanism, and many non-listed species were identified."

**Action:** Text changed to read:

*"Major condensed-phase species were compared to those in the Master Chemical Mechanism (MCM) limonene mechanism, and many non-listed species were identified. The volatility properties of the most prevalent organic nitrates in the produced SOA were determined."*

line 39-40: "The oxidation of VOCs by"

**Action:** Text changed accordingly

line 49: find some more recent refs to add to cite list

**Action:** reference list updated according to reviewer's suggestions

lines 55-58: seems odd not to have the NO<sub>3</sub> + R formation of organonitrates listed here, since this is the one you focus on

**Action/reply:** This reaction is described in text but not in the specific reactions outlined as correctly pointed out by reviewer. However, since all reactions are described in text the reaction mechanism are obsolete and more "text book material". We decided its not necessary to present R1 and R2.

**Action:** Text “Reactions 1–2 show the typical formation pathway of organic nitrates and peroxy nitrates formed from the reactions of NO<sub>x</sub> with RO<sub>2</sub>• originating from a generic VOC, R” and the subsequent reactions has been removed.

line 97 “molecular formulae of major nitrate species produced”

**Action:** Text changed to read “molecular formulae of major nitrate species produced”

line 100 “(based on the Master Chemical. . .”

**Action:** Text changed to read “(based on the Master Chemical Mechanism)”

line 154 “1.4 g cm<sup>-3</sup> (Hallquist. . .” { units}

**Action:** Units have been added

line 167: mention typical [NO<sub>3</sub>] here too, and comment on whether RO<sub>2</sub> + RO<sub>2</sub> or RO<sub>2</sub> + NO<sub>3</sub> reactions should be dominant? in caption for Table 1, mention how you know the [N<sub>2</sub>O<sub>5</sub>]. Can you use these values to get an approximate SOA yield?

**Reply:** If not necessary we prefer to not explicitly present aerosol yields from this flow reactor study since the experimental design was not aimed at that purpose. The amount of N<sub>2</sub>O<sub>5</sub> was assumed to, under dry conditions, be equal to the amount added into the system. [NO<sub>3</sub>] was not measured.

line 210 “silhouette score, s(i) (Rousseuw. . .”

**Action:** Text changed accordingly

around line 236-240: “regions” is confusing – define as the designated mass ranges if you’ll use for further discussion. 237-238 “These regions corresponded to aerosol samples” : what does this mean? They were always enhanced in aerosol samples relative to gas, or . . .?

**Action:** The regions are now better defined as low and high molecular weight regions and connected to monomer and dimer identification. The statement is basically referring to that elevated ion counts were always present in these region for all the aerosol measurements. This is now rephrased:

*“These regions were present in all experiments (Table 1). The occurrence of ions in these regions indicates a prevalence of lower-mass monomer species (typically in the range m/z 340-440) and higher-mass dimer species (typically in the range m/z 580-700).”*

line 245: you refer to specific exptal condition of ratio = 2.4. This sounds contradictory to your statement that the regions “always” correspond to aerosol (I interpreted this as meaning under all ratios of reagents)

**Reply:** We selected ratio 2.4 as one example of all the ratios studied and not a specific exceptional condition. We don’t claim it to be exceptional in the text? Rather we follow up showing the Figure 4 where there is a gradual change in monomer/dimer intensities as the N<sub>2</sub>O<sub>5</sub>/Limonene ratio changes.

**Action:** More clear now after rephrase according to the previous comment.

line 252: you call C11 a dimer? Also, the carbon number ranges here don’t correspond to your shaded regions in Fig. 2, shouldn’t they?

**Reply:** The definition was based on that C11 compounds must be produced from two carbon containing entities. The definition of monomer/dimers has in atmospheric science been used in a

very reluctant way compared to traditional chemistry science, however, we prefer to stick to the more relaxed definition previously used. However, we agree that the carbon numbering does not fit with the figure. Basically, the values are calculated on HR-fit data selected based on carbon number stated while the shading in Figure for simplicity was based on  $m/z$ . We agree this is not consistent.

**Action:** This is now revised and clarified in the text.:

*“From the HR analysis the definition of monomer and dimer was specifically defined based on number of carbons rather than the less strict used of the two  $m/z$  regions illustrated in Fig. 2.”*

line 257: now you’re introducing a new designation, the “first” region for what you’ve called the “monomer” region before (I assume these mean the same thing). I urge you to define a term that refers to these regions at the beginning of this section and stick with it. Even better: label it on Fig. 2.

**Action:** Rephrased to:

*“The lower-mass region, of the two mass-spectra regions (see Fig. 2) typically occurred at  $m/z$  values ranging from 340 to 440 and containing mainly monomers.”*

line 272-273: confused by “at least modestly” ?? wouldn’t this just be the remaining 56.5%? I wouldn’t call that modestly. Or I don’t understand to what you refer here.

**Action:** Text changed to “contributed significantly”

line 274-275: confused by “the monomers contain”: many? all? on average?

**Action:** This sentence is confusing and has been replaced by:

*“One common feature of the monomers without a match in MCM is that they contain a nitrogen atom and have an oxygen number higher than 6, which is a range of compounds that is not represented explicitly in the MCM.”*

line 276: “Progressively more oxygenated monomers of the general . . .”

**Action:** Text now reads “Monomers with progressively more oxygenated monomers of the general formula  $C_{10}H_{15}NO_x$ ”

line 277: omit the paranthetical

**Action:** Parentheses removed

line 283: how would you know a structure is a PAN? Unless you show a mechanism that would get to those species, I’d just leave this discussion as PNs only, they would all readily dissociate.

**Action:** Yes, we agree and have removed the discussion on PAN like compounds as suggested.

line 292: where did the range of formulae you cite for ELVOC come from? Is this your defition, or does it come from Donahue? (similar question for dimer formulae on line 310)

**Action:** Text amended to read “i.e., ELVOCs, which play a key role in SOA formation (Donahue et al., 2012).” At line 310 the formula was removed.

line 299: confused by “using  $\alpha$ -pinene.” using it as what? Nighttime SOA at SOAS is more likely to be from  $\beta$ -pinene, since its  $NO_3$  SOA yields are higher. Not sure what you mean here by invoking  $\alpha$ -pinene.

**Action:** The Lee et al study used lab experiments on  $\alpha$ -pinene to match observations in the field. The sentence has been revised to:

*“The gaseous parent compounds were identified as monoterpenes, matching ions measured in their laboratory study on  $\alpha$ -pinene”*

lines 299-303: rework into one sentence; repetitive; confusing. (Maybe because of trying to tie back to the  $\alpha$ -pin reference? which you could just remove)

**Action:** Shortened and replaced by

*“, enforcing the importance of monoterpene nitrates in the ambient atmosphere.”*

line 304-305: not clear what this sentence means.

**Action:** clarified and now reads:

*“For all elevated ion signals above  $m/z$  390, there was no corresponding product in the MCM mechanism.”*

line 310-311: parenthetical seems internally contradictory: “only” in aerosol phase, but also “slightly about background” in the gas phase?

**Action:** The text has been amended to read

*“(i.e., they were present only in the aerosol phase and at insignificant levels in the gas samples).”*

line 314 “ion families (defined as groups of molecular formulae with only the number of O atoms varying) to the total . . .” {correct?}

**Action:** The text has been amended to read

*“The contributions of the 11 most prevalent ion families (defined as groups of molecular compositions with only the number of O atoms varying) to the total desorbed organic signal are summarized in Table 2.”*

Table 2: the large ranges but with very precise end points for the  $T_{max}$  reported is weird. If you really think only the range is interesting, truncate sig figs. If as I suspect the actual list of  $T_{max}$  values for each member of the family (there are always 6 or fewer, so not too crazy) might be interested to aide your interpretation, why not list them instead, on the order of x value to people can see which correspond? then you can discuss more about which  $T_{max}$ 's appear across monomers / dimers and do some analysis / inference about connectedness from those!

**Action:** The  $T_{max}$  values have been truncated as suggested by the referee.

line 328 “Additionally, (iii) some. . .”

**Action:** Text changed accordingly.

line 346-348: how is this indicative of monomer contributions? do you mean indicative of LOWER monomere contributions to aerosol? Fig 3: why are some traces shaded to zero? describe/ discuss or don't have the difference. in caption, “ $N_2O_5$  ratio” should be “ $N_2O_5$  to limonene ratio” , right?

**Action:** Basically, the compounds with low  $T_{max}$  were also found in the gas-phase and we then suspect them to not be fragments of larger “dimer compounds” but rather being the same compounds in the condensed phase that evaporates without fragmentation. The sentence has been changed to:

*“In general, compounds evaporating at relatively low temperatures were also found in the gas phase, indicative of monomer that partitioning between gas and particle phase.”*

line s 362 / 365: do the “few” and the “ten species” refer to the same subset? This para is confusing.

**Action:** The paragraph has been revised and the part previously starting with “A few monomers.” now reads:

*“Monomer, i.e., lower-mass, species ( $C \leq 10$ ) desorbing at high temperatures could be produced as fragments via thermal degradation of higher-MW species. Some of these ions are matching the chemical composition ( $C_{10}H_{16}O_4$ ,  $C_{10}H_{17}NO_5$ ,  $C_{10}H_{17}NO_6$ , and  $C_7H_{10}O_4$ ) of primary products within the MCM, accounting for (on average)  $69.0 \pm 10.8\%$  of the signal detected in the gas phase. Here some possibilities are plausible, one could be that they are produced as monomer but are important building blocks in the dimer formation, thus thermally decompose back to monomers during desorption.”*

line s 367-369: not sure how / why this suggests favored dimer formation – confusing

**Action:** See point above

line 370: another new designation, “high-MW”! dimer/oligomer? be consistent in how you refer to the different groups

**Action:** Changed to dimer. (oligomer was removed in next sentence)

line 373: cite Figure 4

**Action:** Text now refers to Figure 4

line 374: do you mean “the monomer signal at higher  $N_2O_5$  to limonene ratio”? If so, say so. If not, clarify what you mean

**Action:** The sentence has been modified and now reads:

*“At high ratios of  $N_2O_5$  to limonene, the fraction of dimer species decreased, whereas the percentage of monomer species (fragments) with high  $T_{max}$  increased (Fig. 4).”*

line 375-376: “The average . . . Fig. 4” : remove this sentence, not clear & not helpful, and can cite Fig. 4 above instead.

**Action:** The sentence has been removed

line 407: define oxidation state here, where you first mention it, instead of later where you currently define it Fig. 5: put the labels for mass, desorption temperature, O/C and oxidation state in the same order (1) on the plot, (2) in the caption (and mention all 4!), and put the y axes in the same order, to make life easier on your readers. Also, you show S.D. on the plot (I guess? or, what are the error bars?) – mention this in caption.

**Action:** Oxidation state now defined where first mentioned. The figure has been changed and the reference to SD is now given in the caption.

line 421 do you mean “and are also represented as members of cluster 0”? i.e., the ions are members of both clusters? Clarify.

**Action:** The text now reads

*“This results from the fact that 87% and 69% of cluster 1 and 2 ions, respectively, have secondary thermogram peaks and  $T_{max}$  values, and the ions represented as members of both clusters 1 and 0”*

line s 424-428: Could an alternative rationale for this difference in oxidation state simply be that monomers, because of their small carbon chain length, need more oxidized functional groups to condense, while dimers are so big they'll condense even with less oxidation? Since you are looking only at the aerosol phase here, this pattern could be skewed by differing volatility.

**Action:** Yes, this could be one reason. This alternative rationale is now included in the discussion.

*"It could be that monomers need more oxidation before being transferred into the condensed phase. However, as outlined by the partitioning plots (Fig. S1) most monomers also have a significant condensed phase contribution. Rather, this observation provides some insight into the processes of dimerization that are occurring, indicating the extent to which oxygen is lost during the dimerization process."*

line 437: oxidation state is defined here, should be at first instance of it earlier in text.

**Action:** Oxidation state now defined at first instant.

line 438: @ "certain range of masses", state the range

**Action:** The wording has been changed since there also was a mixup in Figure 5.

*"A positive trend between the Mw and Tmax values, see Fig 5a., was obtained for data in two of the monomer clusters (1 and 2) and the high volatile dimer cluster, while the trend turned negative for the low volatile dimers cluster. It should be noted that monomer species had (in general) higher O/C ratios than the dimers. It could be that monomers need more oxidation before being transferred into the condensed phase. However, as outlined by the partitioning plots (Fig. S1) most monomers also have a significant condensed phase contribution. Rather, this observation provides some insight into the processes of dimerization that are occurring, indicating the extent to which oxygen is lost during the dimerization process."*

line 440: same comment as line s 424-428.

**Action:** ok, see comment on line 424-428

line 445 "during the process, and"

**Action:** This has been extensively revised due to other comments

line 446: as mentioned in general comments above, I think it would be good to include a structural diagram of the HNO<sub>3</sub> leaving reaction.

**Action:** Even if the mechanism on HNO<sub>3</sub> as the leaving group (in a reverse esterification process) is plausible we now after the review comments would be a little bit more cautious. This cautiousness has now been implemented in the manuscript and in line with that we do not want to be explicit in this formation. However, we include that this could be seen as a reverse esterification but also might be linked to observed hydrolysis of organic nitrates (Rindelaub et al, 2015, 2016).

*"The mechanism to create dimers with one nitrogen and a lower O/C ratio would presumably involve the loss of a nitrogen oxides or nitric acid. For this complex system and within the scope of this study it was not possible to firmly proof any mechanism. Since the experiment were done at low RH the direct hydrolysis would be less likely (see Rindelaub et al, 2015, 2016). However, knowing HNO<sub>3</sub> being thermodynamic stable one may speculate in that dimerization of two monomer species via the loss of one HNO<sub>3</sub> molecule could occur e.g. where a C<sub>20</sub>H<sub>29</sub>NO<sub>y</sub> (y = 10–18) species would be generated from*

*C<sub>10</sub>H<sub>15</sub>NO<sub>x</sub> (x = 5–9) species. This process could be seen as the reverse of esterification in order to produce a dimer product with one less nitrogen and reduced numbers of oxygens.*

line s 450 & 452: since this relied on having C9 monomers, it would be useful also to explain how these are formed in the mechanism leading up to dimerization.

**Reply:** There are several pathways for C9 monomer compounds (e.g. 11 MCM compounds has formula C<sub>9</sub>H<sub>14</sub>O<sub>4</sub>). E.g. if both double bonds are oxidized and there is a C-C bond breakage for the exocyclic double bond it will create a C9 monomer. Additional oxygens could be produced by internal H abstractions (e.g. isomerization of RO or RO<sub>2</sub>).

line 453: at the end of this discussion, I think it would also be good to at least mention any alternative possible pathway that could make these dimer products – is it really only possible with HNO<sub>3</sub> loss, or could you get it some other way? Then, perhaps the nitrogen balance or other evidence can help you bolster your hypothesis that the HNO<sub>3</sub> loss is the more likely route.

**Reply/Action:** Yes, there are some suggestions in the literature, however, it is not as clear as one hope it should be and we cannot firmly conclude this so we have to leave that open for speculations and following up-studies on simpler systems. The nitrogen budget would be useful but since HNO<sub>3</sub> is notorious to be “sticky” and we did not measure the other suspected “leaving groups” like NO<sub>2</sub> and NO we have poor handled on this. However, it is clear that the selected dimers only contain one nitrogen and have lower O/C ratio than the sum of the two monomers. Furthermore, the Tmax suggests a high Mw compound (with low vapor pressure) and not a fragment. We now refer to some recent literature on organic nitrate condensed phase reactions (e.g. Rindelaub et al, 2015, 2016) as alternative way to loose nitrogen by hydrolysis.

*“The mechanism to create dimers with one nitrogen and a lower O/C ratio would presumably involve the loss of a nitrogen oxides or nitric acid. For this complex system and within the scope of this study it was not possible to firmly proof any mechanism. Since the experiment were done at low RH the direct hydrolysis would be less likely (see Rindelaub et al, 2015, 2016). However, knowing HNO<sub>3</sub> being thermodynamic stable one may speculate in that dimerization of two monomer species via the loss of one HNO<sub>3</sub> molecule could occur e.g. where a C<sub>20</sub>H<sub>29</sub>NO<sub>y</sub> (y = 10–18) species would be generated from C<sub>10</sub>H<sub>15</sub>NO<sub>x</sub> (x = 5–9) species. This process could be seen as the reverse of esterification in order to produce a dimer product with one less nitrogen and reduced numbers of oxygens.”*

line s 463-464: “dimer fragmentation . . . monomers.” is a confusing sentence

**Action:** Fragmentation has been replaced and the sentence reworded. The sentence now reads:

*“Due to the loss of HNO<sub>3</sub> during dimerization, the potential dimer decomposition during desorption is expected to yield fragments which differ in molecular composition from the precursor (i.e., pre-dimerization) monomers.”*

line s 465-469: can't you demonstrate this more conclusively by looking at specific examples of masses with and without double peaks, and possibly matching up the Tmax's, and thus identify the subset of monomers that are also dissociation products and possibly connect them to precursors? Even better – if relative amounts change with different reaction conditions, can you track them rising and falling together? This dataset would seem to have lots of potential to demonstrate these actually linkages, not just make vague statements and what might / could yield what else upon fragmentation.



**Reply/Action:** In theory, this could be a way forward. However, the complexity and numbers of free parameters will put constraints on such detailed analysis. Actually, the suggestion is very nice but should be done on simpler systems where more solid conclusions on this mechanism could be done. The suggested mechanism is now brought forward with cautiousness and this is now supported with statements on other possible leaving groups and reference to previous work. Hopefully, it will inspire further work on this mechanism.

*“The mechanism to create dimers with one nitrogen and a lower O/C ratio would presumably involve the loss of a nitrogen oxides or nitric acid. For this complex system and within the scope of this study it was not possible to firmly proof any mechanism. Since the experiment were done at low RH the direct hydrolysis would be less likely (see Rindelaub et al, 2015, 2016). However, knowing HNO<sub>3</sub> being thermodynamic stable one may speculate in that dimerization of two monomer species via the loss of one HNO<sub>3</sub> molecule could occur e.g. where a C<sub>20</sub>H<sub>29</sub>NO<sub>y</sub> (y = 10–18) species would be generated from C<sub>10</sub>H<sub>15</sub>NO<sub>x</sub> (x = 5–9) species. This process could be seen as the reverse of esterification in order to produce a dimer product with one less nitrogen and reduced numbers of oxygens.”*

line 480: “obtained for both gas and condensed-phase” – since you don’t discuss gas phase data in this paper, omit, or cite to the companion paper that does study gas phase?

**Action:** Rephrased to state only particle phase

*“High-resolution mass spectrometric data was analysed for condensed-phase reaction products resulting from NO<sub>3</sub> initiated oxidation of the monoterpene, limonene.”*

line 484-485: lots of sig figs on these percentages considering the error bars – better to say 63 +/- 7 and 37 +/- 7 %? And perhaps put a few numbers in the abstract?

**Action:** Number of significant figures has been reduced

line 494-496: this has me wondering whether you can learn anything from the relative intensities of the two peaks? would this pattern support that SOA is “largely determined” by low-volatility oligomers?

**Reply:** If the two peaks are two different compounds with two different formation mechanisms and relative contribution to SOA there is little connection between them as for any pair of compounds detected. So we would not draw those conclusions from these observations.

line 504-505: as mentioned in the general comments, I think you should at least do some discussion of the non-listed products and what they might be.

**Action:** The products that were not found in the MCM list are now marked in the full list found in the supplemental. A comment on these and potential sources are now included.

*“There are two frequently suggested pathways for these. Firstly, the high number of oxygens would be result of isomerization of RO or RO<sub>2</sub> that rarely is described explicit in current modelling framework. Secondly, the presence of di-nitrated compounds relies on secondary chemistry derived from e.g. produced mononitrates intermediates; for limonene containing two double bonds this is more relevant than for other monoterpenes and so far not commonly described in models.”*

line s 509-512: are all the hypothesized HNO<sub>3</sub>-loss dimers in one cluster and others in another? Or, how else can you use the cluster analysis to learn something related to your mechanism speculation?



**Reply:** The cluster analysis clearly separated the fragments from the dimers (obviously, since a fragment cannot be formed according to the mechanism) and also classified the dimers in two groups. However, ions from dimer families containing two nitrogens were found in both clusters. (see Table 2).

**Action:** The explicit statement on the direct link between cluster analysis and the mechanism has been removed.

line 513: "FIGAERO" to be consistent with how you write it above

**Action:** Text changed to read "FIGAERO-CIMS"

line 514: "may provide some means of reducing the complexity. . ." see above general comments. I hope you can work get a bit more out of this.

**Reply:** The changes in the manuscript induced by reviewers have certainly improved the quality of the manuscript and the analysis. Part of this conclusion is hope for some further work to enable a more stringent description on SOA induced from  $\text{NO}_3$  chemistry.

line 520-521: as mentioned above, hard to include species in modeling studies if you haven't even suggested what you think they might be.

**Action:** The compounds are now listed in the supplemental and a short note on potential for extension of model descriptions is given.

*"There are two frequently suggested pathways for these. Firstly, the high number of oxygens would be result of isomerization of RO or RO<sub>2</sub> that rarely is described explicit in current modelling framework. Secondly, the presence of di-nitrated compounds relies on secondary chemistry derived from e.g. produced mononitrates intermediates; for limonene containing two double bonds this is more relevant than for other monoterpenes and so far not commonly described in models."*

## Response to Anonymous Referee #3

This work investigated organic nitrate formation from NO<sub>3</sub> oxidation of limonene. Experiments were conducted using different N<sub>2</sub>O<sub>5</sub>/limonene ratios. Speciated gas and particle phase organic nitrates were measured by the FIGAERO-HR-ToF-CIMS. Cluster analysis of the desorption temperatures of organic nitrate species resulted in five clusters; the relationships between O/C, OS, MW, etc of these clusters were discussed. Formation of dimers was observed and reaction mechanisms for dimer formation were proposed.

This is an interesting study and the manuscript is generally well-written and easy to follow. This study will be of interest to the greater atmospheric community. My main comments are 1) while the experiments were conducted over a range of N<sub>2</sub>O<sub>5</sub>/limonene ratios, the authors shall provide more context to this experimental design. Also, the results from experiments with different N<sub>2</sub>O<sub>5</sub>/limonene ratios need to be more extensively and clearly discussed. 2) I have some concerns regarding the discussion of the results shown in Fig. 5, please see details below. 3) There are a number of recent studies on nitrate radical oxidation of biogenic hydrocarbons, it would be appropriate that these studies are referenced in the manuscript to reflect the current state of knowledge. Overall, I recommend publication in ACP once these comments are addressed. Most comments are mainly to improve clarity of the manuscript.

### Main Comments

1. Page 5 line 158. Are potential impurities (e.g., NO<sub>2</sub> and HNO<sub>3</sub>) in the N<sub>2</sub>O<sub>5</sub> synthesized measured and quantified? Please make this clear in the manuscript.

**Action:** This is now clarified in the experimental:

*“N<sub>2</sub>O<sub>5</sub> was synthesized by reacting ≥20 ppm O<sub>3</sub> with pure NO<sub>2</sub> (98%, AGA Gas) in a glass vessel and then passing the flow through a cold trap maintained at -78.5 °C using dry ice. Even if neither HNO<sub>3</sub> nor NO<sub>2</sub> was measured it is known from previous work that this method typically provides a source with impurities less than a few percent. It is well known that the resulting white solid would show signs of yellowing, due to nitric or nitrous acid contamination, if exposed to moisture (e.g., ambient lab air) so handling of the N<sub>2</sub>O<sub>5</sub> was done accordingly.”*

2. Page line 168. What is the reason for performing experiments with different N<sub>2</sub>O<sub>5</sub>/limonene ratios? Please provide more context here.

**Reply:** It would reflect a gradual increase in reaction of the exocyclic double bond. At a ratio of 1:1 we expect NO<sub>3</sub> to primarily react with the exocyclic double bond, representing the typical case producing primary products, while increasing the ratio will add more possibilities for reactions also with the endocyclic double bond, reflecting secondary atmospheric chemistry.

**Action:** Added text in experimental:

*“At a ratio around 1.0 one expects only the endocyclic double bond to be reacting with NO<sub>3</sub> radicals while at higher ratio there is an increased possibility for secondary chemistry where products will be susceptible for reaction with the NO<sub>3</sub> radical.”*

3. Page 6 Table 1. a. With these N<sub>2</sub>O<sub>5</sub>/limonene ratios, are all limonene (and both double bonds?) reacted away? Please clarify and change the “limonene” in the table to either “reacted limonene” or “initial limonene”. b. What is the RO<sub>2</sub> reaction regime in these experiments? RO<sub>2</sub> + NO<sub>3</sub>? RO<sub>2</sub> + RO<sub>2</sub>? c. Can SOA yields be quantitatively calculated from the values in the table? If the “limonene” is reacted limonene, the SOA yields appear to be very low compared to previous studies by Fry et al. (ACP, 2009), Fry et al. (ACP, 2011), and Boyd et al. (ES&T, 2017). Please discuss the results from this study in the context of these prior studies. Also, do the data shown in Table 1 follow a typical Odum 2- product yield curve?

**Reply:** If not necessary we prefer not to explicitly present aerosol yields from this flow reactor study. The experiments were not designed to derive yields.

4. Page 8 line 238. It was noted that “. . .the relative signal intensities varied with the amount of limonene and N<sub>2</sub>O<sub>5</sub> present in the system”. I think the authors are referring to Fig. 4? Please add the figure number to the sentence to help guide the readers if this is the case.

**Reply:** Yes, the referee is right but we then realize that this figure would then be introduced too early in the manuscript.

**Action:** We have removed the statement

*“and the relative signal intensities varied with the amount of limonene and N<sub>2</sub>O<sub>5</sub> present in the system.”*

5. Page 8 line 260. It is not immediately clear what these species are without diving into the entire MCM mechanisms. The authors should at least include the formation mechanisms of these major ions in the SI to help guide the readers. Also, it would be helpful to propose mechanisms for the major species that were observed in this study but are not in MCM. On the related note, Boyd et al. (ES&T, 2017) recently expanded the limonene + NO<sub>3</sub> mechanisms in MCM. It might be worthwhile to evaluate if some species detected in this study are covered in the expanded mechanism in Boyd et al.

**Reply:** The Boyd et al. paper was unfortunately not available when the majority of the analysis in the present study was done.

**Action:** We have referred to the Boyd et al, study. Even if we here and there refer to MCM compounds we have made it easier by listing MCM compounds in the full list of the 198 ions identified (supplemental). Furthermore, in addition to the described dimer mechanism speculation we summaries the general pathway for mechanism developments by including the following statements:

*“The non-listed species (see Table S1) were either dimer species or more highly oxygenated, nitrated analogs of known major products, which are notoriously hard to describe via standard gas-phase mechanisms. There are two frequently suggested pathways for these. Firstly, the high number of oxygens would be result of isomerization of RO or RO<sub>2</sub> that rarely is described explicit in current modelling framework. Secondly, the presence of di-nitrated compounds relies on secondary chemistry derived from e.g. produced mononitrates intermediates; for limonene containing two double bonds this is more relevant than for other monoterpenes and so far not commonly described in models.”*

6. Page 9 line 280. What are some of the mechanisms for limonene and its oxidation products to react with NO<sub>2</sub> and HNO<sub>3</sub>?

**Reply:** The possibilities are for example that NO<sub>2</sub> could react with peroxy-radicals and HNO<sub>3</sub> might do condensed phase nitration. We don't think that this of general value and would not add that.

7. Page 10 line 293. Nah et al. (ES&T 2016) also measured a large suite of highly oxygenated organic nitrates from NO<sub>3</sub> oxidation of  $\alpha$ -pinene and  $\beta$ -pinene in laboratory experiments, using the FIGAERO-HR-ToF-CIMS. Many of those are also observed in Lee et al. (PNAS, 2016).

**Reply:** We have noted the request for including Nah et al. (ES&T 2016).

**Action:** As the last sentence in this paragraph we added:

*"Complementary, Nah et al. (2016) also measured a large suite of highly oxygenated organic nitrates from NO<sub>3</sub> oxidation of  $\alpha$ -pinene and  $\beta$ -pinene in laboratory experiments."*

8. Page 10 line 299. It is noted that "The similarity with ions from the NO<sub>3</sub>-initiated limonene oxidation further emphasizes the importance of monoterpenes as precursors of organic nitrates". It would be informative if the authors indicate in the Table in SI (the ion list) regarding which ions have also been observed in the ambient (Lee et al.) and other monoterpene experiments (Nah et al).

**Reply:** We would prefer to focus on comparison with limonene studies. It turns out there is now a parallel study by Boyl et al, 2017 (accepted when this manuscript was submitted) that could be better suited for comparisons.

9. Page 10 line 301. Rollins et al. (Science, 2012) discussed the importance of limonene + NO<sub>3</sub> in a field study.

**Action:** This reference has now been added in the instruction. This part has been reduced, as a consequent of other comments, and do not refer to the importance of limonene+NO<sub>3</sub>

10. Page 12 line 362. It was noted that there is a positive correlation (R<sup>2</sup> = 0.67) between T<sub>max</sub> and molecular mass. Are the authors referring to Fig 5a? If so, it does not look like the overall correlation is that good? Please clarify.

**Reply/action:** Yes, it referred to Fig5a. However, its better to have that discussion later in the paper so we removed the statement here and extended/clarified the text later to read.

*"A positive trend between the Mw and T<sub>max</sub> values, see Fig 5a., was obtained for data in two of the monomer clusters (1 and 2) and the high volatile dimer cluster, while the trend turned negative for the low volatile dimers cluster."*

11. Page 13 line 370-379. (this is also related to comment #2 above). It is not clear to me how the higher N<sub>2</sub>O<sub>5</sub>/limonene experiments lead to formation of more thermally unstable mechanisms. Please explain. More discussions are needed here, to provide context to why experiments are

conducted with different N<sub>2</sub>O<sub>5</sub>/limonene in the first place and why/how the resulting compositions are different.

**Reply:** This is discussed in the above #2 comment

12. Page 13 Figure 4. What is the function used for the fit? Is this just to guide the eye or there is a fundamental reason for such a dependence?

**Reply:** yes, we agree the line is mostly for guidance of the eye and the r<sup>2</sup> should be removed.

**Action:** The r<sup>2</sup> has been removed. The end of the Figure caption now reads:

*“The lines indicated are for the guidance of the eye.”*

13. Page 15, discussions of Figure 5. The authors attempted to discuss the relationships between O/C, OS, and MW, etc. However, within uncertainties, there do not seem to be significant differences in the O/C and OS values for all clusters. Hence, this discussion needs to be revised.

a. (related to comments # 2 and 11 above). In Figure 5, will any specific patterns emerge if the authors only look at the data from experiment of a particular N<sub>2</sub>O<sub>5</sub>/limonene ratio?

b. line 418. It was noted that the O/C of cluster 0 is similar to clusters 1 and 2. However, within the uncertainties, the O/C ratios of all clusters are almost the same.

c. line 426, should the high-MW clusters be (3,4)? And the low-MW clusters be (0, 1, 2)?

d. line 427. It was noted that the ions in the high-MW clusters have a lower OS than ions in clusters 0-3. Firstly, should “0-3” be “0-2”? Secondly, it does not look like the high-MW clusters have a lower OS. Within uncertainties, the OS values appear to be the same for all clusters.

e. line 434. It was noted that a positive correlation exists between O/C and T<sub>max</sub>. It is not clear how this is case from the data shown in Fig. 5c. Please provide a figure and show the R<sup>2</sup> value.

**Action/replies:**

- a) Figure 5 describes a cluster analysis that requires multiple data and cannot be compared with single experiments. Generally, the same features are found for individual experiments. However, there is a gradual change when changing the N<sub>2</sub>O<sub>5</sub>/limonene as illustrated in Fig 4.
- b) The SD is not necessary described as an uncertainly but rather the variability in each property. It’s a clear and significant shift in the median for each property even if the clusters have overlapping variability.
- c) Yes, text changed accordingly
- d) Yes, typo changed. For uncertainty discussion see b)
- e) The figure has been mixed up. Intention was to describe the trends in Fig 5a, i.e. Mw vs T<sub>max</sub>. The text has been changed and now reads:  
*“A positive trend between the Mw and T<sub>max</sub> values, see Fig 5a., was obtained for data in two of the monomer clusters (1 and 2) and the high volatile dimer cluster, while the trend turned negative for the low volatile dimers cluster.”*

## Minor Comments

1. Page 2 line 44. Would be appropriate to reference Ng et al. (ACP, 2017).

**Action:** Reference has been added

2. Page 2 line 46. Would be appropriate to also reference Day et al. (AE, 2010); Fry et al. (ACP, 2013); Xu et al. (PNAS, 2015); Xu et al. (ACP, 2015); Boyd et al. (ACP, 2015); Kiendler-Scharr et al. (GRL, 2016); Nah et al. (ES&T, 2016).

**Action:** References have been added

3. Page 2 line 60. Delete “M” in front of Hallquist.

**Action:** The “M.” has been removed

4. Page 3 line 77. Boyd et al. (ES&T, 2017) recently investigated SOA formation from NO<sub>3</sub> oxidation of limonene.

**Action:** Reference has been added

6. Page 14 Figure 5. Missing y-axis label for 5b?

**Action:** This is fixed now.

# Characterization of organic nitrate constituents of secondary organic aerosol (SOA) from nitrate radical-initiated oxidation of limonene using High-Resolution Chemical Ionization Mass Spectrometry

Cameron Faxon<sup>1</sup>, Julia Hammes<sup>1</sup>, Ravi Kant Pathak<sup>1</sup>, Mattias Hallquist<sup>1</sup>

<sup>1</sup>Department of Chemistry and Molecular biology, University of Gothenburg, Göteborg, SE-41258, Sweden

**Abstract:** The gas phase nitrate radical ( $\text{NO}_3^*$ ) initiated oxidation of limonene can produce organic nitrate species with varying physical properties. Low-volatility products can contribute to secondary organic aerosol (SOA) formation and organic nitrates may serve as a  $\text{NO}_x$  reservoir, which could be especially important in regions with high biogenic emissions. This work presents the measurement results from flow reactor studies on the reaction of  $\text{NO}_3^*$  with limonene using a High-Resolution Time-of-Flight Chemical Ionization Mass Spectrometer (HR-ToF-CIMS) combined with a Filter Inlet for Gases and AEROSols (FIGAERO). Major condensed-phase species were compared to those in the Master Chemical Mechanism (MCM) limonene mechanism, and many non-listed species were identified. The volatility properties of the most prevalent organic nitrates in the produced SOA were determined. Analysis of multiple experiments resulted in the identification of several dominant species (including  $\text{C}_{10}\text{H}_{15}\text{NO}_6$ ,  $\text{C}_{10}\text{H}_{17}\text{NO}_6$ ,  $\text{C}_8\text{H}_{11}\text{NO}_6$ ,  $\text{C}_{10}\text{H}_{17}\text{NO}_7$ , and  $\text{C}_9\text{H}_{13}\text{NO}_7$ ) that occurred in the SOA under all conditions considered. Additionally, the formation of dimers was consistently observed and these species resided almost completely in the particle phase. The identities of these species are discussed, and formation mechanisms are proposed. Cluster analysis of the desorption temperatures corresponding to the analyzed particle-phase species yielded at least five distinct groupings based on a combination of molecular weight and desorption profile. Overall, the results indicate that the oxidation of limonene by  $\text{NO}_3^*$  produces a complex mixture of highly oxygenated monomer and dimer products that contribute to SOA formation.

## 1 Introduction

Oxidation of gas-phase organic species contribute significantly to particle formation and growth (Hallquist et al., 2009; Smith et al., 2008; Wehner et al., 2005), and thus a thorough understanding of secondary organic aerosol (SOA) formation mechanisms is important for the accurate estimation of its impact on the climate system (Kanakidou et al., 2005).

Secondary organic aerosols form primarily via the photooxidation of volatile organic compounds (VOCs), yielding less volatile products, which can then partition into the condensed phase (Hallquist et al., 2009; Kroll and Seinfeld, 2008), especially when pre-existing aerosols (e.g., inorganic seed particles) are present (Kroll et al., 2007). The products resulting from atmospheric oxidation may be classified as low volatility, semi-volatile, and intermediate volatility OCs, i.e., LVOCs, SVOCs, and IVOCs, respectively (Donahue et al., 2012; Jimenez et al., 2006; Murphy et

Deleted: -

Deleted: and

Deleted: identified, and the identity and

Deleted: The observed and expected (listed) products (associated with the Master Chemical Mechanism (MCM) limonene mechanism) were compared, and many non-listed species were identified.

45 al., 2014). In addition, extremely low volatility OCs (i.e., ELVOCs) contribute significantly to  
 46 aerosol formation and early growth (Ehn et al., 2014; Jokinen et al., 2015). The oxidation of  
 47 VOCs by the primary atmospheric oxidants, O<sub>3</sub> and ·OH, has been extensively investigated (Cao  
 48 and Jang, 2008; Hallquist et al., 2009; Kanakidou et al., 2005; Kroll and Seinfeld, 2008).  
 49 Although less studied than the photo-oxidation of VOCs, the reaction of VOCs with the nitrate  
 50 radical (NO<sub>3</sub>·) and the resulting formation of organic nitrates are also important, especially for  
 51 nocturnal chemistry (Roberts, 1990; Brown and Stutz, 2012; Perring et al., 2013; Kiendler-  
 52 Scharr et al., 2016; Ng et al., 2017). Significant concentrations of these nitrates have been  
 53 detected in the gas and condensed phases in both field and laboratory studies (Ayres et al., 2015;  
 54 Beaver et al., 2012; Boyd et al., 2017; Bruns et al., 2010; Day et al., 2010; Fry et al., 2013; Lee et  
 55 al., 2016; Nah et al., 2016; Paulot et al., 2009; Rindelaub et al., 2014, 2015, Rollins et al., 2012,  
 56 2013; Xu et al., 2016; Kiendler-Scharr et al., 2016).

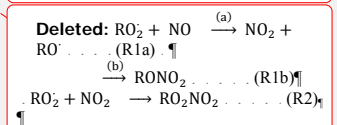
Deleted: photo-

Deleted: Roberts, 1990).

Deleted: ).

57 Organic nitrates (RONO<sub>2</sub>) and organic peroxy nitrates (RO<sub>2</sub>NO<sub>2</sub>), such as peroxy acetyl  
 58 nitrate (PAN), may also form in the atmosphere (Roberts, 1990; Singh and Hanst, 1981; Temple  
 59 and Taylor, 1983). RO<sub>2</sub>NO<sub>2</sub> may form via the reaction of organic peroxy nitrates (RO<sub>2</sub>·) with  
 60 NO<sub>2</sub>, while RONO<sub>2</sub> may form directly through either the reaction of RO<sub>2</sub>· with NO or the  
 61 reaction of unsaturated VOCs with NO<sub>3</sub>·.

Deleted: Reactions 1–2 show the typical formation pathway of organic nitrates and peroxy nitrates formed from the reactions of NO<sub>3</sub> with RO<sub>2</sub>· originating from a generic VOC, R



Deleted: M.

62 Secondary organic aerosol-precursor VOCs arise mainly from the emission and reaction of  
 63 biogenic VOCs (BVOCs) (Hallquist et al., 2009), with up to 90% of the global VOC budget  
 64 originating from biogenic sources (Glasius and Goldstein, 2016; Guenther et al., 1995). Isoprene,  
 65 the main constituent of global BVOC terrestrial emissions (600 Tg yr<sup>-1</sup>) (Guenther et al., 2006), is  
 66 highly reactive with ·OH, O<sub>3</sub>, and NO<sub>3</sub>· (Atkinson et al., 1995; Hallquist et al., 2009). However,  
 67 monoterpenes typically have higher SOA yields than isoprene (Carlton et al., 2009; Presto et al.,  
 68 2005b) and regarding atmospheric emissions, α-pinene, β-pinene, and limonene constitute the  
 69 main monoterpenes emitted into the atmosphere (Guenther et al., 2012). In addition to its high  
 70 emission rates, limonene is especially interesting as a model BVOC, due to its relatively high  
 71 reaction rates (Ziemann and Atkinson, 2012) and occurrence in indoor environments, owing to  
 72 emission sources, such as air fresheners and other household products (Wainman et al., 2000).

73 The reactions and mechanisms of α-pinene and β-pinene oxidation have been more  
 74 thoroughly studied (Bonn and Moorgat, 2002; Presto et al., 2005a, 2005b; Fry et al., 2009;  
 75 Perraud et al., 2010) than those associated with limonene. Several studies have focused on the  
 76 ozonolysis of and SOA formation from limonene (Leungsakul et al., 2005; Jonsson et al., 2006,  
 77 2008a; Zhang et al., 2006; Baptista et al., 2011; Sun et al., 2011; Pathak et al., 2012; Jiang et al.,  
 78 2013; Youssefi and Waring, 2014). NO<sub>3</sub>· oxidation of limonene and the resulting organic nitrates  
 79 that may contribute to SOA formation have, however, rarely been investigated (Hallquist et al.,  
 80 1999; Spittler et al., 2006; Fry et al., 2011, 2014; Boyd et al., 2017). In relation to the reaction with  
 81 NO<sub>3</sub>·, major non-nitrate products of limonene (including endolim) have been identified, but  
 82 significant SOA formation was preceded by the occurrence of multiple unidentified nitrates  
 83 (Hallquist et al., 1999; Spittler et al., 2006). Moreover, although mechanistic models and

Deleted: ; Presto et al., 2005a, 2005b

Deleted: Baptista

Deleted: 2011; Jiang et al., 2013

Deleted: Leungsakul

Deleted: 2005

Deleted: Sun

Deleted: 2011

Deleted: ; Zhang et al., 2006).

Deleted: Fry et al., 2011, 2014;



107 molecular identities of these products have been proposed, direct measurement and identification  
108 thereof have yet to be reported. Further elucidation of the mechanisms governing and products  
109 generated by the reactions of limonene and  $\text{NO}_3^*$  are warranted, since organic nitrates from  
110 BVOCs (including limonene) have been consistently observed in field studies (Perring et al.,  
111 [2009](#); Ayres et al., 2015; Beaver et al., 2012; Lee et al., 2016, 2014b),

Deleted: ; Perring et al., 2009).

112 Additionally, the contribution of low-volatility products to the SOA mass may increase  
113 with the formation of dimers from aerosol components generated by VOC oxidation. Numerous  
114 dimers or oligomers have been found in SOA generated by monoterpene species (e.g.  
115 Emanuelsson et al., 2013; Kourtchev et al., 2014, 2016; Kristensen et al., 2016; Müller et al.,  
116 2007; Tolocka et al., 2004). However, the speciation of observed dimers and oligomers from  
117 organic nitrates, especially with respect to detailed formation mechanisms, has rarely been  
118 reported.

119 Here we report the chemical composition of low-volatility gas and aerosol-phase species,  
120 formed from mixtures of  $\text{N}_2\text{O}_5$  and limonene, as measured by a High Resolution Time-of-Flight  
121 Chemical Ionization Mass Spectrometer (HR-ToF-CIMS) coupled to a Filter Inlet for Gases and  
122 AEROSols (FIGAERO) inlet (Lopez-Hilfiker et al., 2014). The objectives of this work were  
123 three-fold namely, to: (i) determine the molecular formulae, of major nitrate species, produced  
124 from the reaction of limonene with  $\text{NO}_3^*$ , that could contribute significantly to SOA formation  
125 and growth, (ii) compare the distribution of measured products to that of the expected products  
126 (based on, the Master Chemical Mechanism (MCM)) to identify any discrepancies in the  
127 mechanistic understanding of nitrate formation from limonene, and (iii) categorize, via cluster  
128 analysis, the thermodynamic desorption data measured for selected condensed-phase species.

Deleted: formula

Deleted: ,

Deleted: formed via

## 129 2 Methods

### 130 2.1 Experimental setup

131 Experiments were performed in the Gothenburg Flow Reactor for Oxidation Studies at  
132 low Temperatures (GFROST) at the University of Gothenburg. In previous studies, this facility  
133 was used for studying the impact of relative humidity, OH-scavengers, and temperature on SOA  
134 formation via monoterpene ozonolysis (Emanuelsson et al., 2013; Jonsson et al., 2008a, 2008b),  
135 its volatility properties (Pathak et al., 2012), and dimer formation during the ozonolysis of  $\alpha$ -  
136 pinene (Kristensen et al., 2016). The inflow of zero air and the reagents is fixed at a total flow of  
137 1.6 L per min (LPM). The experiments are all run at low RH ( $\leq 1\%$ ) and a constant temperature of  
138  $20^\circ\text{C}$ . To catch only the center portion of the laminar flow and avoid unnecessary interference  
139 from wall effects, samples are taken through a cone at the end of the reactor at 0.95 LPM. The  
140 average residence time of the sampled portion of the mixture is 240 s. Due to the flow  
141 restrictions, a make-up flow of zero air is added to the sample, immediately after the outlet, prior  
142 to being sampled by the instruments. The amount of dilution flow necessary is constrained by the  
143 flow required by the HR-ToF-CIMS. Figure 1 shows a diagram of the experimental setup.

144

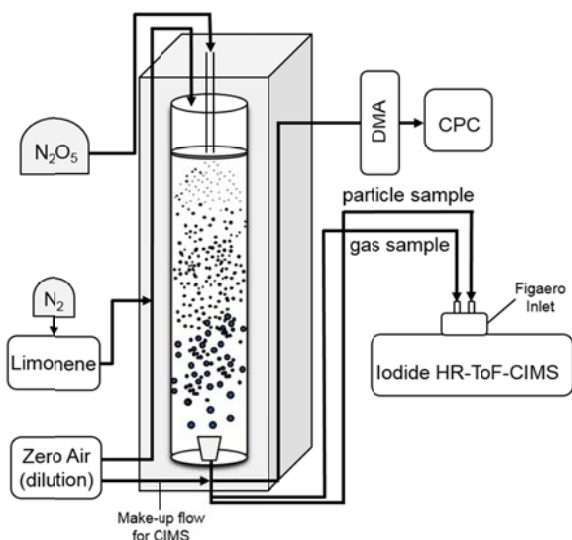


**Figure 1.** Diagram of experimental setup of GFROST during experiments.

149  
150

153 Gas and particle-phase products were measured using a High-Resolution Time-of-Flight  
 152 Chemical Ionization Mass Spectrometer (HR-ToF-CIMS) coupled to a Filter Inlet for Gases and  
 153 AEROSols (FIGAERO) (Lopez-Hilfiker et al., 2014). The HR-ToF-CIMS can be operated in  
 154 either negative- or positive-ionization modes, using various reagent-ion sources. CIMS  
 152 measurement techniques have previously been employed for the measurement of organic nitrate  
 158 products of monoterpenes (Beaver et al., 2012; Paulot et al., 2009) using multiple reagent ions  
 157 (Lee et al., 2014a). In this work, the HR-ToF-CIMS was operated using negative Iodide ( $I^-$ ) ion  
 158 as the reagent in all experiments. Dry UHP  $N_2$  was passed over a permeation tube containing  
 155 liquid  $CH_3I$  (Alfa Aesar, 99%), and  $I(H_2O)_n^-$  ions were generated by directing the flow over a  
 167  $^{210}Po$  radioactive source. Reaction products (e.g., species  $X$ ) were identified by their  
 163 corresponding cluster ions,  $XI^-$ , thereby allowing the collection of whole-molecule data. The  
 162 reagent and sample flowed into the Ion-Molecule Reaction (IMR) chamber of the instrument at a  
 163 nominal individual rate of 2 LPM. The IMR was temperature-controlled at  $40^\circ C$  and operated at  
 164 a nominal pressure of 200 mbar. With  $I^-$  ionization, the sensitivity of a detected species (i.e.,  $Hz$   
 162  $ppt^{-1}$ ) can vary significantly with relative humidity (Lee et al., 2014a). However, the experiments  
 166 were all performed at low RH ( $\leq 1\%$ ) and, hence, the same sensitivity was realized for all the  
 167 conditions considered.

168 The FIGAERO inlet was used during the experiments, and particles were collected on a  
 165 Zeffluor® PTFE membrane filter. The aerosol sample line and gas sample line were composed of  
 176 12 mm copper tubing and 12 mm Teflon tubing, respectively. The inlet was operated in regular  
 177 cycles – 1 h of gas-phase sampling and simultaneous particle collection, followed by a 1-h period  
 173 where the filter was shifted into position over the IMR inlet and the collected SOA was desorbed.  
 179 Desorption was facilitated by a 2 LPM flow of heated UHP  $N_2$  over the filter. The temperature of

174 the N<sub>2</sub> was increased from 20 to 200°C in 50 min (3.5°C min<sup>-1</sup>), and a subsequent 10-minute  
175 temperature soak was performed to ensure complete removal of the remaining organic material  
176 that volatilizes at 200°C. The measured species were distinguished based on their thermal  
177 properties via the resulting desorption time-series profiles, hereafter referred to as thermograms.  
178 Temperature gradients of >3.5°C min<sup>-1</sup> have been used in previous studies, but, in this work, a  
179 lower gradient was used to enable optimum thermal separation (Lee et al., 2014a; Lopez-Hilfiker  
180 et al., 2014). The HR-ToF-CIMS was configured to measure singly charged ions with a mass-to-  
181 charge ratio (*m/z* or *Th*) of 7–720. Particles were contemporaneously sampled directly at the  
182 outlet of the flow reactor, through a ¼" stainless steel 1 m sample line, by a Scanning Mobility  
183 Particle Sizer (SMPS). The SMPS measured the number-size distribution used for estimating the  
184 mass concentrations, based on the assumption of spherical particles with a density of 1.4 g cm<sup>-3</sup>  
185 (Hallquist et al., 2009). In all cases, SOA was generated via nucleation and growth rather than by  
186 using seed particles.

187 ~~N<sub>2</sub>O<sub>5</sub> was synthesized by reacting ≥20 ppm O<sub>3</sub> with pure NO<sub>2</sub> (98%, AGA Gas) in a glass~~  
188 ~~vessel and then passing the flow through a cold trap maintained at -78.5°C using dry ice. Even if~~  
189 ~~neither HNO<sub>3</sub> nor NO<sub>2</sub> was measured it is known from previous work that this method typically~~  
190 ~~provides a source with impurities less than a few percent. It is well known that the~~ resulting white  
191 solid ~~would show~~ signs of yellowing, due to nitric or nitrous acid contamination, ~~if~~ exposed to  
192 moisture (e.g., ambient lab air) ~~so handling of the N<sub>2</sub>O<sub>5</sub> was done accordingly~~. The solid N<sub>2</sub>O<sub>5</sub>  
193 was transferred to a diffusion vial fitted with a capillary tube (inner diameter: 2 mm). The N<sub>2</sub>O<sub>5</sub>  
194 diffusion source was held at a constant temperature (-23 °C), and the gravimetrically determined  
195 mass loss rate remained steady (*r*<sup>2</sup> value: 0.97–0.98) for several weeks. A similarly characterized  
196 d-limonene (Alfa Aesar, 97%) diffusion source was held at temperatures ranging from 8.5 to  
197 31.5°C and, using Gas Chromatography–Mass Spectrometry (GC-MS; Finnigan/Tremetrics),  
198 diluted flow-reactor concentrations (15, 45, 92, and 150 ppb).

199 Experiments were performed over a range (1.0–113) of N<sub>2</sub>O<sub>5</sub>/limonene ratios (see Table 1  
200 for a summary of experimental conditions). ~~At a ratio around 1.0 one expects only the endocyclic~~  
201 ~~double bond to be reacting with NO<sub>3</sub> radicals while at higher ratio there is an increased~~  
202 ~~possibility for secondary chemistry where products will be susceptible for reaction with the NO<sub>3</sub>~~  
203 ~~radical~~. For each set of conditions in the flow reactor, sampling was performed over a period of  
204 6–12 h to ensure stability of conditions (e.g., gas-phase signals, total SOA mass) and repeatability  
205 of the FIGAERO thermal-desorption cycles. ~~An example of three sequential desorptions is shown~~  
206 ~~in Fig. S2~~.

207

Deleted: 2.2 Reagent preparation¶

Deleted: by

Deleted: The

Deleted: showed

Deleted: only when

Deleted: ).

Deleted: ).

Table 1. Experimental conditions considered in this study.

#	N <sub>2</sub> O <sub>5</sub> (ppb)	Limonene (ppb)	N <sub>2</sub> O <sub>5</sub> /Limonene	Average SOA Mass* ( $\mu\text{g m}^{-3}$ )
3	95	15	6.3	12 $\pm$ 2
4	95	15	6.3	8 $\pm$ 1
2	95	40	2.4	8 $\pm$ 1
5	95	40	2.4	10 $\pm$ 1
6	95	95	1	12 $\pm$ 1
1	160	15	10.7	8 $\pm$ 1
11	850	95	8.9	25 $\pm$ 2
12	850	150	5.7	47 $\pm$ 2
7	1700	15	113.3	7 $\pm$ 1
8	1700	40	42.5	11 $\pm$ 1
9	1700	95	17.9	43 $\pm$ 2
10	1700	150	11.3	95 $\pm$ 3

\*Errors are given as standard deviation of the measured mean.

216

217

218

## 2.2. CIMS data-analysis methods

Data obtained from the HR-ToF-CIMS was analyzed using the Tofware (Tofwerk/Aerodyne) analysis software written in Igor Pro (WaveMetrics). High-resolution analysis allowed for ion identification with a resolution of  $\sim 4000$  ( $m/\Delta m$ ). Identified species were cross-checked with predicted species generated via the MCM v3.3.1 limonene mechanism (Saunders et al., 2003) and the corresponding theoretical product distribution was compared with the measured distribution for both gas and particle phase. For several ions, product formulas in the MCM were used as the major parameter for ion identification at a given  $m/z$ . However, this identification scheme resulted in the misidentification of several ions. The identification of high-mass ions ( $m/z > 500$ ) was complicated by the fact that the number of possible formulas increases rapidly with increasing mass and carbon number of the ions. Nevertheless, the high accuracy of fits ( $\leq 5$  ppm), where the identities of expected product ions were corroborated by the fits of expected isotopes, reduced uncertainties stemming from the mass calibration and provided reliable ion identifications. To further ensure the accuracy of the identities of high-mass ions, the fits of the identified ions were compared over all experiments.

The high-resolution ion data was further analyzed with Python 3.5.2 using the pandas (McKinney, 2010, 2011) and NumPy (Van Der Walt et al., 2011) packages, and peaks in the ion thermograms were identified using an implementation of the PeakUtils package (v1.0.3, <http://pythonhosted.org/PeakUtils/>). For each experiment, the temperature ( $T_{\text{max}}$ ) corresponding to the peak signal of each ion observed during the desorption of SOA particles was identified. Furthermore, a secondary temperature ( $T_{\text{max},2}$ ) was identified when double-peak behavior was observed.

240

Deleted:

Deleted: 1

... [1]

Deleted: .0

Deleted: 11

... [2]

Deleted: 3

Deleted: .

### 2.3 Cluster-analysis methods

Deleted: 4

Cluster analysis, performed via the K-Means algorithm (scikit-learn machine learning package; Pedregosa et al., 2011), was used to distinguish, based on their elemental composition and thermodynamic behavior ( $T_{\max}$ ), groups of ions observed during SOA desorption. This algorithm, utilizing a random seeding approach (Arthur and Vassilvitskii, 2007), was chosen due to the superior cluster separation realized after comparing several algorithms, including affinity propagation and mean-shift clustering. The solution of the K-Means algorithm is obtained through the minimization of an inertia function (see Eq. 1)  $\Phi$ , which is equivalent to the sum of the mean-squared distance between all samples and their corresponding cluster centroid,  $c$  (Arthur and Vassilvitskii, 2007; Raschka, 2016). Here,  $x^{(i)}$ : sample (e.g., carbon number, oxygen number,  $T_{\max}$ ) in a set of  $n$  samples,  $c^{(j)}$ : cluster center of cluster  $j$  in a set of  $k$  clusters, and  $w^{(i,j)}$ : weighting coefficient ( $w^{(i,j)} = 1$  if  $x^{(i)}$  is in cluster  $j$ ,  $w^{(i,j)}=0$  otherwise).

$$\phi = \sum_{i=1}^n \sum_{j=1}^k w^{(i,j)} \|x^{(i)} - c^{(j)}\|^2 \quad (1)$$

The quality of the cluster separation was assessed through a silhouette score,  $s(i)$  (Rousseeuw, 1987), which allows comparison of the intra-cluster and inter-cluster distances and, for a sample  $i$ , is determined from:

$$s(i) = \frac{b(i) - a(i)}{\max\{a(i), b(i)\}} \quad (2)$$

where,  $a(i)$ : average distance, or dissimilarity, between point  $i$  and each point within its own cluster and  $b(i)$ : average dissimilarity between point  $i$  and all points within the nearest neighboring cluster. The value of  $s(i)$  ranges from -1 to 1 and reflects the quality of the clustering with respect to the separation between members of each cluster. For example, a score of ~1 indicates that the point is relatively far away from the nearest neighboring cluster, while a score of 0 suggests that the cluster separation is roughly equivalent to that of cohesion clusters; that is,  $a(i) \approx b(i)$ . For all points within a clustered dataset, an average silhouette score can indicate the adequacy of the cluster separation for a given number of clusters.

Detected ions were clustered based on their molecular weight (MW), elemental numbers ( $n_C$ ,  $n_H$ ,  $n_O$ ,  $n_N$ ), and  $T_{\max}$  values. Compared with the other variables, MW and the carbon number exhibited the highest correlation with  $T_{\max}$ . Clustering the ions based on these three variables yielded the best separation with respect to mass and  $T_{\max}$  of the ions. Input variables were scaled to values between 0 and 1 (based on their respective range of input values) to prevent any bias associated with the relative magnitude of each variable (e.g.,  $MW \gg n_C$ ).

278

## 280 3 Results and discussion

### 281 3.1 Characterization of mass spectra from SOA and identification of species

282 Products in both the gas and condensed phases were identified by analyzing HR-ToF-  
283 CIMS data collected under various experimental conditions (Table 1). In each sampling regime,  
284 major products were readily identifiable, and only modest or negligible fragmentation occurred  
285 with application of the soft ionization technique. The focus in the current work was on condensed  
286 phase products using the FIGARO inlet desorption. Recently, Stark *et al.* (2017) showed that  
287 fragmentation during the desorption can occur within the FIGAERO. In the current work the  
288 fragmentation within the FIGARO was not specifically investigated. However, from our cluster  
289 analysis it was evidently that fragmentation occurred with specific features in e.g. molecular  
290 weight and evaporation temperature. The ramp rate during desorption was therefore maintained  
291 for all experiments to ensure, if fragmentation did occur, it would be consistent and enable  
292 comparable analysis of the dataset. The mass-to-charge ( $m/z$  or Th) values of the most prominent  
293 ions of species detected in the collected aerosol were determined from the average mass spectra  
294 obtained during desorption cycles. The results revealed two distinct regions consisting of several  
295 clusters of elevated ion signals (Fig. 2). These regions were present in all experiments (Table 1).  
296 The occurrence of ions in these regions indicates a prevalence of lower-mass monomer species  
297 (typically in the range  $m/z$  340-440) and higher-mass dimer species (typically in the range  $m/z$   
298 580-700). These results are analogous to those of previous ozonolysis studies, where highly  
299 oxygenated multifunctional (HOM) molecules from monoterpene oxidation were observed using  
300 a nitrate HR-ToF-CIMS (Ehn *et al.*, 2014; Jokinen *et al.*, 2015; Mentel *et al.*, 2015). Figure 2  
301 shows an average mass spectrum corresponding to four sequential 1-h desorption cycles of 12- $\mu\text{g}$   
302  $\text{m}^{-3}$  SOA samples from a reaction mixture with a  $\text{N}_2\text{O}_5$  to limonene ratio of 2.4. The gas to  
303 particle ratio of most ions were below one as illustrated in Fig. S1, whereas the focus of this work  
304 was to characterize the particle phase.

305 In total, 198 of the identified organic ions constituted significant fractions of the aerosol  
306 samples, but most of the signal emanated from only ~25% of these species. The dominant species  
307 were identified by averaging the desorption-time series of all experiments and extracting the top  
308 75<sup>th</sup> percentile (by averaging the signal during desorption) of the monomer and dimer ions. The  
309 resulting set of ions consisted of 52 molecular species that accounted for 76% of the organic  
310 signal during desorption, while the top 90<sup>th</sup> percentile of ions (20 ions) accounted for 56%. This  
311 52-ion set consisted of 28 monomers ( $C = 7-10$ ) and 24 dimers or oligomers ( $C = 11-20$ ). From  
312 the HR analysis the definition of monomer and dimer was specifically defined based on number  
313 of carbons rather than the less strict used of the two  $m/z$  regions illustrated in Fig. 2. On average,  
314 the top 75<sup>th</sup> percentile of monomers and the top 75<sup>th</sup> percentile of dimers accounted for 83% of  
315 the total monomer signal and 70% of the total dimer signal, respectively. A full list of ions and  
316 the composition of the 40<sup>th</sup>, 75<sup>th</sup>, and 90<sup>th</sup> percentile subsets can be found in the Supplementary  
317 Information (Table S1). This list is based on a common sensitivity for detection that might not  
318 always be true and highly variable (see e.g. Isaacman-Van Wertz *et al.*, 2017). However, with this  
319 assumption the list will provide molecular identity of the most prominent organic compounds

Deleted: corresponded to aerosol samples considered in

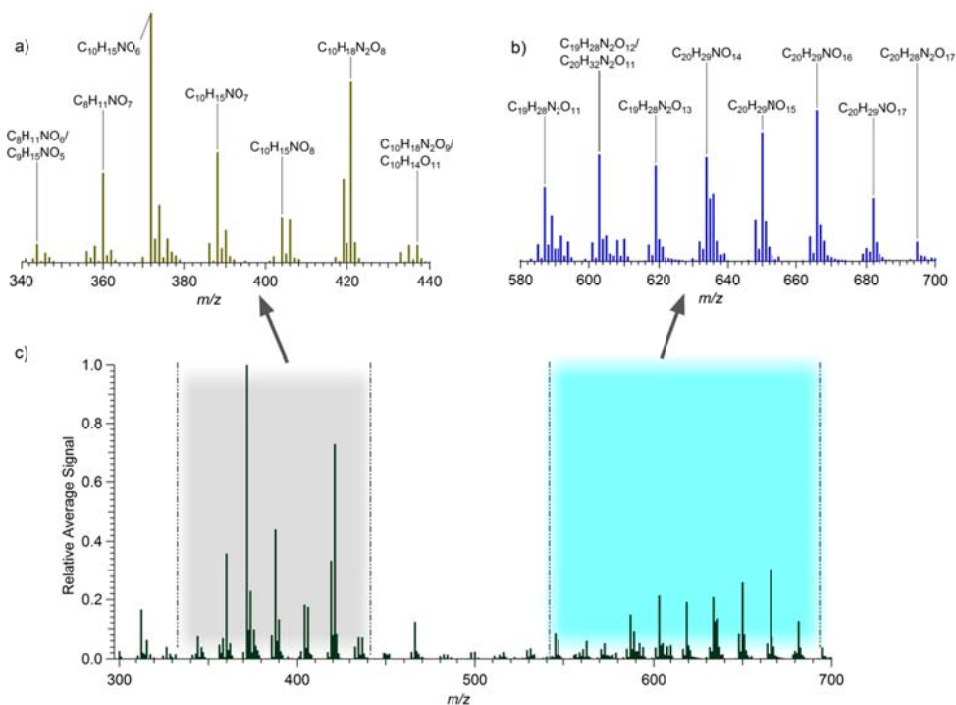
Deleted: ), and the relative signal intensities varied with the amount of limonene and  $\text{N}_2\text{O}_5$  present in the system.

Deleted: and

Deleted: .

321 contributing to the SOA mass outlined in Table 1. One could assess the contribution of these  
322 peaks to the total mass loading, although with high variation in molecular mass and oxidation, the  
323 sensitivity is likely to vary significantly, resulting in large error margins and therefore deeming  
334 any interpretation highly speculative.

339 The lower-mass region, of the two mass-spectra regions (see Fig. 2) typically occurred at  $m/z$   
332 values ranging from 340 to 440 and containing mainly monomers. Several ions in this region  
331 matched the predicted molecular formulas associated with the MCM limonene mechanism, and  
332 the largest signals occurred for species consisting of 8–10 carbon atoms. E.g. the dominant ions  
333 occurring at  $m/z$  360, 372, 374, and 390 (during desorption) corresponded to the iodide-cluster  
334 ions  $C_8H_{11}NO_7I$ ,  $C_{10}H_{15}NO_6I$ ,  $C_{10}H_{17}NO_6I$ , and  $C_{10}H_{17}NO_7I$  (Fig. 2a). These correspond to the  
335 MCM species C727PAN and C731PAN, C923PAN, NLIMALOH and LIMALNO3,  
336 NLIMALOOH, respectively.



339 **Figure 2.** Representative average mass spectrum for the desorption of SOA collected during the experiments:  
346 Identification of ions detected in the (a) monomer region ( $m/z$  340–440) and (b) dimer region ( $m/z$  580–700). (c)  
345 Relative intensities and positions of the two regions detected in all aerosol samples. Data was obtained from four 1-h  
347 desorption cycles of  $12\text{-}\mu\text{g m}^{-3}$  samples from a mixture with a  $N_2O_5$ /limonene ratio of 2.4. The un-clustered (i.e., not  
343 clustered with I<sup>-</sup>)  $m/z$  of each ion is  $-127 m/z$ .  
349

347 Elevated signals of monomer ions (e.g.,  $C_{10}H_{15}NO_7$  ( $m/z$  388),  $C_{10}H_{15}NO_8$  ( $m/z$  404),  
348  $C_{10}H_{17}NO_8$  ( $m/z$  406), and  $C_{10}H_{15}NO_9$  ( $m/z$  420)), which are absent from the list of expected

Deleted: .

Deleted: first, i.e.,

Deleted: 350

Deleted: 450



351 products of the mechanism, also occurred in this region. These non-MCM species contributed  
352 significantly to the total organic monomer signal, and MCM species accounted for only  $43.5 \pm$   
353  $3.2\%$  of the total monomer signal of all experiments. One common feature of the monomers  
354 without a match in MCM is that they contain a nitrogen atom and have an oxygen number higher  
355 than 6, which is a range of compounds that is not represented explicitly in the MCM.

356 Monomers with progressively more oxygenated monomers of the general formula  
357  $C_{10}H_{15}NO_x$  were detected for  $x = 5-9$  i.e.,  $C_{10}H_{15}NO_5-C_{10}H_{15}NO_9$  with  $C_{10}H_{15}NO_6$  being the  
358 dominant species in both the aerosol and gas phase in most experiments. Ions with molecular  
359 formulas containing two nitrogen atoms, for example,  $C_{10}H_{16}N_2O_8$  ( $m/z$  419) and  $C_{10}H_{18}N_2O_8$   
360 ( $m/z$  421), were also detected (Fig. 2a). Limonene and its primary products reacted only with  
361  $NO_2$ ,  $NO_3^*$ , and  $HNO_3$ , yielding molecules that are most likely di-nitrate species, with additional  
362 functional groups. E.

363 Similar to the highly oxygenated multi-functional species (HOMs) resulting from the  
364 ozonolysis of monoterpenes (Ehn et al., 2014; Jokinen et al., 2015), including limonene, many of  
365 the observed species could be classified as extremely low-volatility organic compounds (i.e.,  
366 ELVOCs, which play a key role in SOA formation (Donahue et al., 2012)). Observations  
367 performed under ambient conditions during the 2013 Southern Oxidant and Aerosol Study  
368 (SOAS) revealed the presence of highly functionalized particulate organic nitrates containing 6–8  
369 oxygen atoms (Lee et al., 2016). In that work, these species constituted 3% and 8% of sub- $\mu m$   
370 aerosol mass during daytime and nighttime hours, respectively, and exhibited a distinct diurnal  
371 pattern, typically reaching peak concentrations between midnight and the early-morning hours.  
372 The gaseous parent compounds were identified as monoterpenes, matching ions measured in their  
373 laboratory study on  $\alpha$ -pinene, enforcing the importance of monoterpene nitrates in the ambient  
374 atmosphere. Complementary, Nah et al. (2016) also measured a large suite of highly oxygenated  
375 organic nitrates from  $NO_3$  oxidation of  $\alpha$ -pinene and  $\beta$ -pinene in laboratory experiments.

376 For all elevated ion signals above  $m/z$  390, there was no corresponding product in the  
377 MCM mechanism. As shown in Fig. 2b, zooming into  $m/z$  580-700 illustrating the high mass  
378 dimer region, the largest ion signals corresponded to compounds with 19 and 20 carbons in the  
379 dimer region.  $C_{20}H_{22}N_2O_8$  and  $C_{20}H_{29}NO_{17}$ , which occurred at significantly elevated levels in all  
380 aerosol samples, constituted the lowest- and highest-mass dimers, respectively (see Fig. 2 for  
381 other examples of  $C_{19}$  and  $C_{20}$  dimer species). Many of these can be considered ELVOC species  
382 based on their respective formulas and their partitioning behavior (i.e., they were present only in  
383 the aerosol phase and at insignificant levels in the gas samples).  $C_{19}H_{28}N_2O_x$  and  $C_{20}H_{29}NO_x$  were  
384 the most dominant families of  $C_{19}$  and  $C_{20}$  dimers, respectively. Taken together, 10 individual  
385 dimers from these two families were identified in all experiments.

386 The contributions of the 11 most prevalent ion families (defined as groups of molecular  
387 compositions with only the number of O atoms varying) to the total desorbed organic signal are

Deleted: , at least modestly,

Deleted: In contrast to the MCM species,

Deleted: one

Deleted: more than six

Deleted: atoms

Deleted: species

Deleted: (

Deleted: ,

Deleted: )

Deleted: Some of the measured species could either be peroxy nitrates or similar in structure to peroxy acetyl nitrate (PAN). PAN-like species readily undergo thermal degradation (Orlando et al., 1992; Tuazon et al., 1991; Wooldridge et al., 2010) at temperatures significantly lower than those (100–200°C) used to heat the samples. Therefore, the number of intact PAN-like ions reaching the detector could be significantly diminished relative to their prevalence in the collected aerosol. However, the measured ions with a given formula may consist of peroxy-nitrates, di-nitrates, and PAN-like species.

Deleted: ELVOC, with the general formula  $C_{10}H_{14-16}O_{7-11}$ ,

Deleted: using

Deleted: . The similarity with ions from the  $NO_3^*$ -initiated limonene oxidation further emphasizes

Deleted: monoterpenes as precursors of organic nitrates. Furthermore, the occurrence of such compounds

Deleted: environment reinforces the notion that the formation of the

Deleted: limonene-derived organic nitrate species detected, here, is important to the troposphere

Deleted: Through the MCM mechanism, Deleted: occurred without formation of the

Deleted: products.

Deleted: (e.g.,  $C_{19-20}H_{28-32}O_{10-18}$  for dimers)

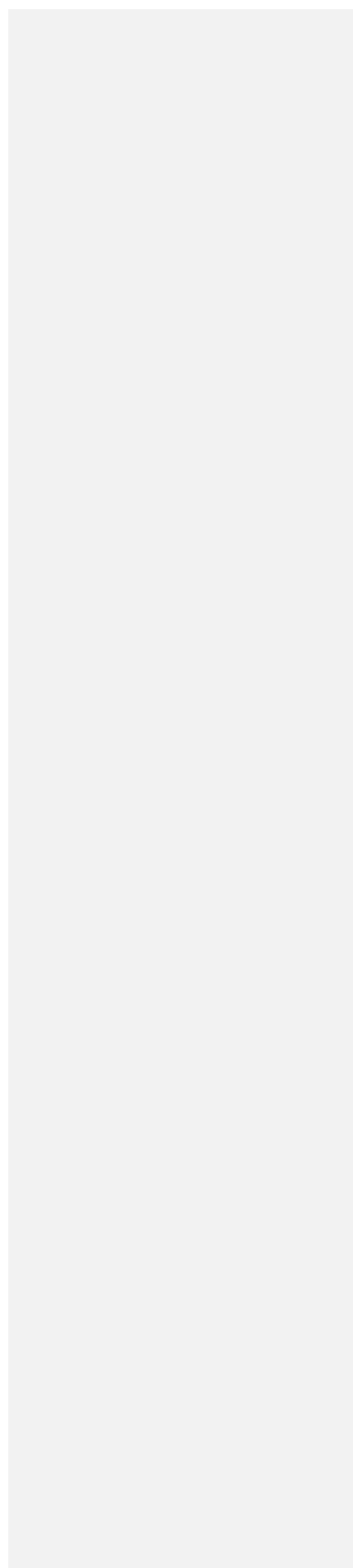
Deleted: occurred

Deleted: ,

Deleted: slightly above background



435 summarized in Table 2. Average contributions are calculated from the mean signals for each  
436 family relative to the total mean organic signal generated during all experiments.  
437  
438



439 **Table 2.** Peak desorption temperature ( $T_{\max}$ ) and the average contribution (over all experiments) to the organic signal  
 440 during SOA desorption for the most commonly observed product families. The number of monomer species in each  
 441 family that desorbed at only high temperatures is noted in parentheses.

Class	#	Family	# Observed in Family	Average Contribution	$T_{\max}$ Range ( $^{\circ}\text{C}$ )
Monomers	m1	C10H15NO <sub>x</sub>	5 (1)	23.0 ± 8.0 %	74 – 152
	m2	C10H18N2O <sub>x</sub>	2 (0)	8.8 ± 2.4 %	66 – 70
	m3	C10H16N2O <sub>x</sub>	5 (1)	6.7 ± 2.2 %	52 – 154
	m4	C10H17NO <sub>x</sub>	5 (2)	5.3 ± 2.7 %	59 – 159
	m5	C8H11NO <sub>x</sub>	3 (0)	4.7 ± 1.4 %	68 – 81
	m6	C9H13NO <sub>x</sub>	4 (0)	3.0 ± 1.1 %	70 – 75
	m7	C9H15NO <sub>x</sub>	4 (0)	2.0 ± 0.7 %	64 – 76
Dimers	d1	C20H29NO <sub>x</sub>	4	7.1 ± 3.3 %	100 – 154
	d2	C19H28N2O <sub>x</sub>	6	5.0 ± 2.2 %	101 – 157
	d3	C20H27NO <sub>x</sub>	4	2.8 ± 1.2 %	101 – 151
	d4	C20H24N2O <sub>x</sub>	3	2.0 ± 1.7 %	125 – 157

442

### 443 3.2 Characterization of identified ions via thermal properties

444 The desorption data is characterized by the frequent occurrence of multiple peaks  
 445 corresponding to certain ions, and the thermograms in all experiments reveal four characteristic  
 446 desorption patterns, which exhibit the following trends: (i) from 45 to 85°C, some monomer  
 447 species undergo almost complete desorption. (ii) Some monomers yield two peaks - one in the  
 448 low-temperature range and another at significantly higher temperatures. Additionally, (iii) some  
 449 monomer ions, associated with certain individual species of the monomer families, occurred at  
 450 only very high desorption temperatures, owing possibly to the fragmentation of high-mass  
 451 oligomers and dimers. (iv) Although less prominent than that observed for monomers, a double  
 452 peak occurred for several dimers, whereas for other dimers a single primary desorption peak  
 453 occurred at mid to high temperatures (110–170°C). The occurrence of multiple peaks is  
 454 consistent with the thermal degradation of extremely low-volatility species that desorb only at  
 455 temperatures >200°C. Similar behavior has been observed in previous studies (Holzinger et al.,  
 456 2010; Lopez-Hilfiker et al., 2014, 2015; Yatawelli et al., 2012), where the secondary peaks  
 457 observed during desorption were attributed to the thermal degradation of very low-volatility  
 458 aerosol components.

459 Analysis of the desorption profiles (thermograms) may yield additional information about  
 460 the properties of each detected chemical species. The gradual heating of the FIGAERO filter  
 461 from 25°C to 200°C resulted in a clear volatility-based separation of species and, for each ion  
 462 detected, the desorption temperature corresponding to the maximum signal was identified.

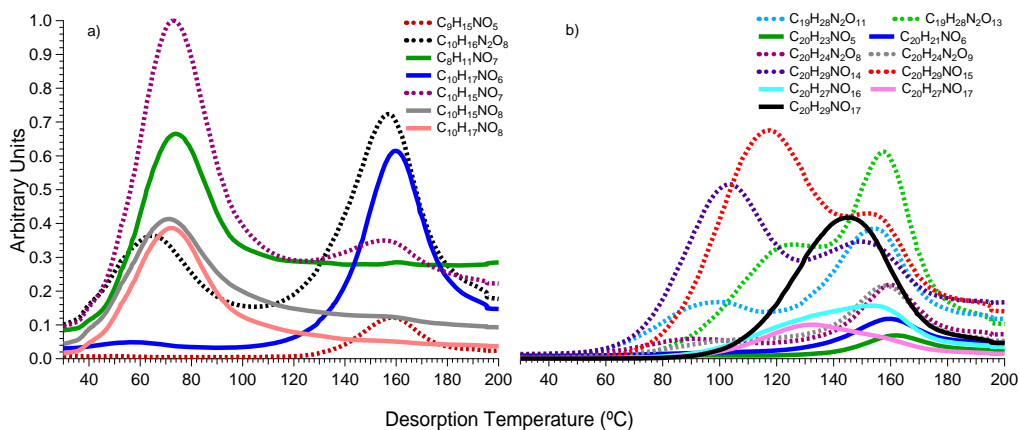
Deleted: (N/C)×10
Deleted Cells
Deleted: 1.0
Deleted: .7
Deleted: .4
Deleted: 2.0
Deleted: .3 – 69.8
Deleted: 0
Deleted: 6.7%
Deleted Cells
Deleted: 51.9
Deleted: .0
Deleted: 1.0
Deleted Cells
Deleted: 58.7
Deleted: .2
Deleted: 1.3
Deleted: 67.5 – 80.5
Deleted: 3.0%
Deleted Cells
Deleted: .4 – 74.5
Deleted: 1.1
Deleted Cells
Deleted: 63.9 – 75.7
Deleted: 0.5
Deleted: .2
Deleted: .0
Deleted: 1.1
Deleted: .1 – 156.9
Deleted: 0.5
Deleted: 100.5
Deleted: .3
Deleted: 0
Deleted: 2.0%
Deleted: 124.5 – 156.9
Deleted Cells

493 Furthermore, the average desorption temperature of the monomer species was typically lower  
 494 than that of their dimer counterparts, which are less volatile. Higher masses (than those  
 495 associated with the monomer species) were typically desorbed from the FIGAERO filter at higher  
 496 temperatures. An example of this characteristic behavior is shown in the average thermograms  
 497 (Fig. 3) of several monomer and dimer ions. In general, compounds evaporating at relatively low  
 498 temperatures were also found in the gas phase, indicative of monomer that partitioning between  
 499 gas and particle phase.

Deleted: constituted significant fractions of

Deleted: contributions to the aerosol

500  
501



502  
503

504 **Figure 3.** Average thermograms (over four desorption cycles) for an  $N_2O_5$  ratio of 2.4. Thermograms of ion clusters  
 505 of the (a) monomer species ( $C_8$ – $C_{10}$ ) and (b) dimer ( $C_{19}$ – $C_{20}$ ) species. Ions with double-peak thermogram shape  
 506 patterns, consistent with the fragmentation of low-volatility oligomers, are shown as dashed lines.

507

508 As shown in Fig. 3, each of the detected ion signals reaches at least one local maximum  
 509 value. The temperature at which a signal reached the first maximum ( $T_{max}$ ) value was similar  
 510 across all experiments (average standard deviation: <10%). Secondary peaks occurred more  
 511 frequently for species with a carbon number of 10 or lower, consistent with a degradation-based  
 512 contribution. Although the temperature at which the secondary local maximum occurs ( $T_{max,2}$ )  
 513 provides insight into the occurrence of dimerization, the  $T_{max}$  value was taken as the true  
 514 desorption temperature of each ion.

515  $T_{max}$  values were identified for each ion in the 196-ion set. Monomer, i.e., lower-mass,  
 516 species ( $C \leq 10$ ) desorbing at high temperatures could be produced as fragments via thermal  
 517 degradation of higher-MW species. Some of these ions are matching the chemical composition

Deleted:

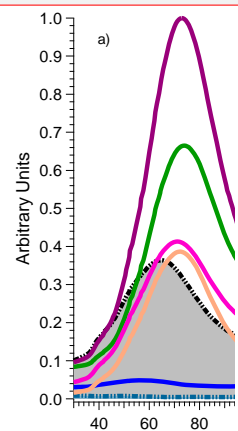
Deleted: highlighted

Deleted: , and (in general) a positive correlation ( $r^2 = 0.67$ ) was obtained for the dependence of  $T_{max}$  on the molecular mass. A few monomer

Deleted: may have formed (

Deleted: ) mainly as fragments rather than as primary reaction products and, therefore, desorbed only at high temperatures. However, four

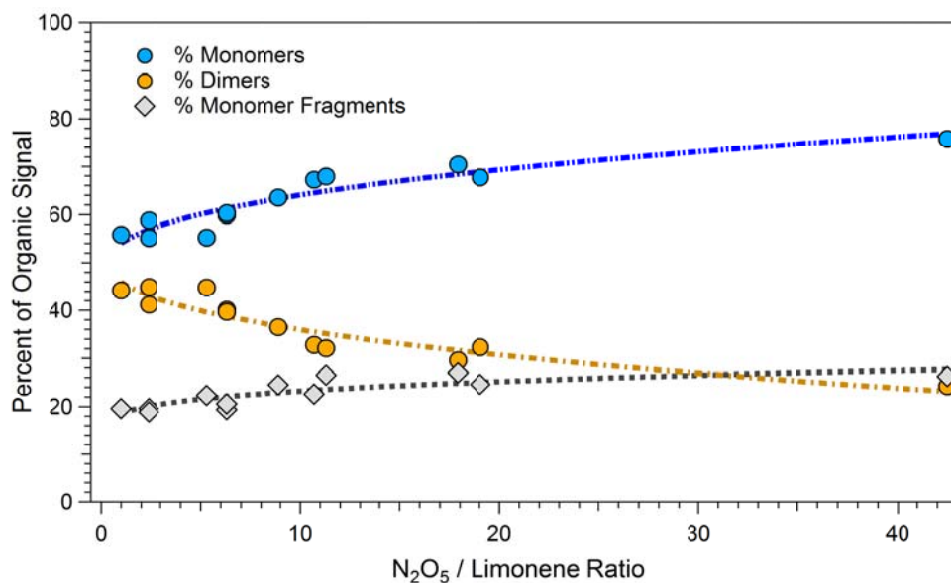
Deleted: ten species



533 (C<sub>10</sub>H<sub>16</sub>O<sub>4</sub>, C<sub>10</sub>H<sub>17</sub>NO<sub>5</sub>, C<sub>10</sub>H<sub>17</sub>NO<sub>6</sub>, and C<sub>7</sub>H<sub>10</sub>O<sub>4</sub>) of primary products within the MCM,  
 539 accounting for (on average) 69.0 ± 10.8% of the signal detected in the gas phase. Here some  
 539 possibilities are plausible, one could be that they are produced as monomer but are important  
 539 building blocks in the dimer formation, thus thermally decompose back to monomers during  
 532 desorption.

536 The ratio of dimer to monomers varied between experiments. At high ratios of N<sub>2</sub>O<sub>5</sub> to  
 537 limonene, the fraction of dimer species decreased relative to the total organic signal, whereas the  
 546 percentage of high-temperature desorbing monomer species (fragments) increased (Fig. 4). This  
 549 suggests that absolute dimer formation may have remained the same, but the monomer signal is  
 542 over-represented by monomer fragments generated from high-mass, thermally unstable  
 541 compounds. This percentage is calculated based on the assumption of a common detection  
 542 sensitivity across all ions; this assumption may influence the estimated (percentage) contribution  
 543 of monomers relative to that of dimers.

547



543  
 544 **Figure 4.** Percentage of monomer, dimer, and high-temperature monomer signal (observed during desorption)  
 542 relative to the ratio of N<sub>2</sub>O<sub>5</sub> to limonene injected into the reactor. The data points at a ratio of 113 are not shown (22,  
 546 78, 39%, respectively). The lines indicated are for the guidance of the eye.

552

553 **3.3 Characterization of major SOA products via cluster analysis**

Deleted: occurred as

Deleted: This suggests

Deleted: under

Deleted: investigated N<sub>2</sub>O<sub>5</sub> to limonene ratios,

Deleted: from these monomer species (which also evaporate as fragments)

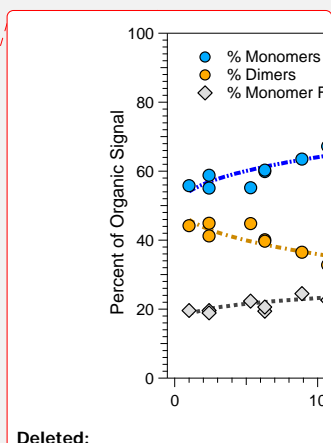
Deleted: ) is highly favored.

Deleted: high-MW species

Deleted: and oligomer

Deleted: .

Deleted: The average percentages of particle-phase monomers and dimers relative to the ratio of reactants across all experiments are shown in Fig. 4.

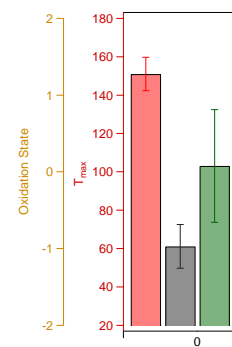
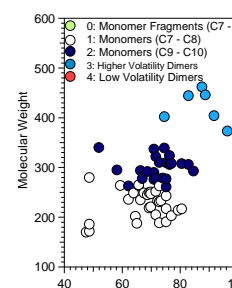


569 Clustering was performed on an ion set consisting of 117 ions, which accounted for >90%  
570 of the total organic signal generated during desorption in all experiments. Ions generating  
571 extremely low signal (i.e. the thermogram did not exhibit any structure identifiable above  
572 background noise prohibiting Tofware to constrain a mathematical fit for  $T_{max}$  calculations) were  
573 excluded to prevent analysis of ions with mis-identified  $T_{max}$  values. However, the occurrence of  
574 high-temperature desorbing monomer outliers (described previously) and the double-peak  
575 behavior exhibited by several monomers rendered the mass- and temperature-based grouping of  
576 these ions difficult. To address this issue, duplicate entries, corresponding to  $T_{max}$  and  $T_{max,2}$ ,  
577 were assigned to all ions exhibiting double-peak behavior, allowing the clear separation and  
578 analysis of low-mass ions desorbing at temperatures >120°C.

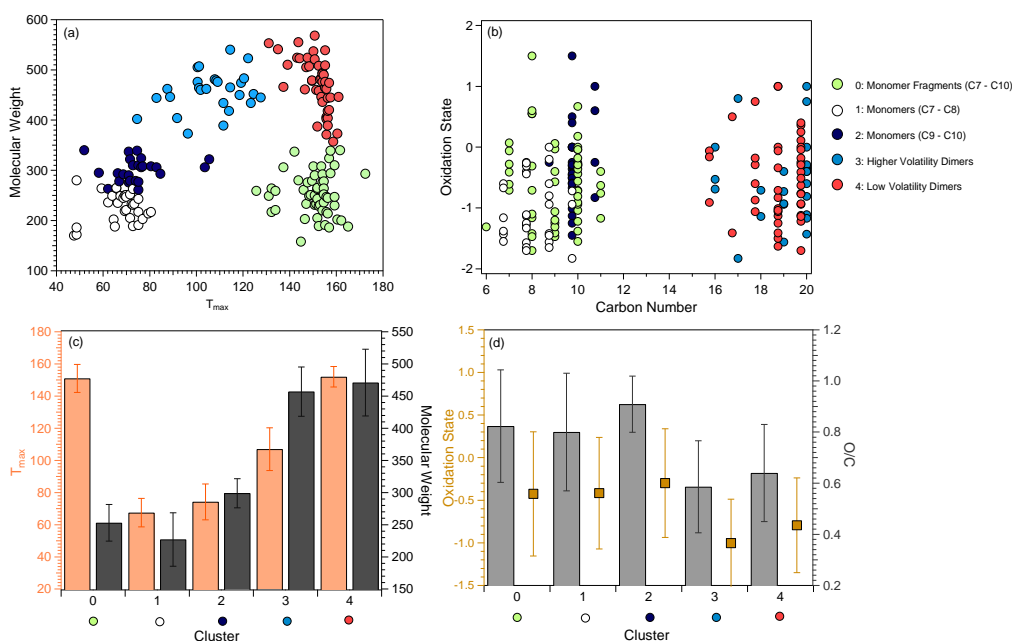
579 Four and five clusters ( $\#_{clust} = \{4, 5\}$ ), using  $T_{max}$ , MW, and #C as input, yielded the best  
580  $T_{max}$ -based clustering and separation of ions. The use of  $n_H$  and  $n_O$  as additional input parameters  
581 resulted in partial separation of clusters into groups with similar O/C and H/C ratios, and poor  
582 correlations with respect to  $T_{max}$ . The average silhouette score obtained for four clusters was  
583 better (0.81 vs. 0.72) than that obtained for five clusters. However, the use of five clusters  
584 allowed for the separation of low-temperature desorbing monomers into two groups with distinct  
585 average  $T_{max}$ , and MW with smaller differences in O/C ratios, and oxidation states ( $2 \times O/C - H/C$   
586  $- 5 \times N/C$ ). Using more than five clusters resulted in a further decrease in the quality of cluster  
587 separation, as measured by the inertia (Eq. 1) and average silhouette score (Eq. 2). Although the  
588 identification of subgroups within each cluster are possible by increasing  $\#_{clust}$ , the five main  
589 clusters were chosen based on their separation by mass and  $T_{max}$  values and to reduce complexity  
590 of the interpretation of the resulting clusters with respect to the chemical composition.

591 Figure 5a shows the cluster separation on the MW- $T_{max}$  plane. The distribution of  
592 individual cluster members based on oxidation states and #C (Fig. 5b), and the mean MW,  $T_{max}$ ,  
593 O/C, and oxidation state of each cluster (Fig. 5c) are also shown.

Deleted: .



Deleted:



596

597 **Figure 5.** Characteristics of the five identified clusters: (a) Desorption temperature of each observed ion in the top  
 598 40<sup>th</sup> percentile of ions (identified by their respective desorption signal), color-coded by their corresponding cluster  
 599 number, (b) Oxidation state relative to carbon number of all observed ions, colored by their corresponding cluster  
 600 membership (for visualization purposes, carbon numbers of groups 0, 2, and 4 are offset), (c) average cluster mass  
 601 and desorption temperature, and (d) average cluster oxidation state and O/C ratios. Error bars in panels (c) and (d)  
 602 indicate standard deviations for each cluster property.

603

604 As Fig. 5 shows, the five clusters are characterized by distinct average MWs and  
 605 corresponding average  $T_{max}$  values. Cluster 0 consists of monomer ions, which are considered  
 606 fragments of larger, less-volatile molecules that desorb at high temperatures. The average  
 607 oxidation state and O/C ratio are similar to those of clusters 1 and 2, which are composed  
 608 primarily of C7–C9 and C9–C10 monomer ions, respectively. This results from the fact that 87%  
 609 and 69% of cluster 1 and 2 ions, respectively, have secondary thermogram peaks and  $T_{max}$  values,  
 610 and the ions represented as members of both clusters 1 and 0. Ions corresponding to the identified  
 611 dimers are contained in clusters 3 and 4. The dimers are characterized by two primary desorption  
 612 regimes, with species that desorb at mid-range temperatures (80–130°C) occurring in cluster 3  
 613 and the highest-mass, lowest-volatility ions occurring in cluster 4. Moreover, the distribution of  
 614 individual cluster members with respect to #C and oxidation state (Fig. 5b) shows that members  
 615 of low-MW clusters (0, 1, 2) and high-MW clusters (3, 4) reside in separate regimes. The ions in  
 616 high-MW clusters have a significantly larger number of carbon atoms per molecule and, hence,  
 617 lower (on average) oxidation states than ions in clusters 0–2. With respect to the most prevalent

Deleted: and

Deleted: Average

Deleted: properties with respect to

Deleted: ,

Deleted: ,

Deleted: are

Deleted: cluster

Deleted: high

Deleted: low

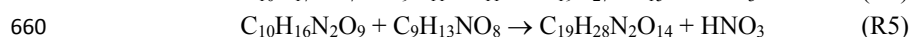
Deleted: 3

628 families listed in Table 2, monomer families m2, m3, and m4 reside exclusively in cluster 2,  
629 whereas m5 and m7 reside exclusively in cluster 1. Family members of m1 and m6 were split  
630 20/80% and 75/25% between clusters 1 and 2, respectively. Dimer families d1–d4 occurred  
631 predominantly (66–75%) in cluster 4, with the remainder residing in cluster 3. None of the dimer  
632 families in Table 2 occurred in clusters 0, 1 or 2.

633 A positive trend between the M<sub>w</sub> and T<sub>max</sub> values, see Fig 5a, was obtained for data in  
634 two of the monomer clusters (1 and 2) and the high volatile dimer cluster, while the trend turned  
635 negative for the low volatile dimers cluster. It should be noted that monomer species had (in  
636 general) higher O/C ratios than the dimers. It could be that monomers need more oxidation before  
637 being transferred into the condensed phase. However, as outlined by the partitioning plots (Fig.  
638 S1) most monomers also have a significant condensed phase contribution. Rather, this  
639 observation provides some insight into the processes of dimerization that are occurring,  
640 indicating the extent to which oxygen is lost during the dimerization process.

### 641 3.4 Mechanisms of dimerization

642 The mechanism to create dimers with one nitrogen and a lower O/C ratio would  
643 presumably involve the loss of a nitrogen oxides or nitric acid. For this complex system and  
644 within the scope of this study it was not possible to firmly proof any mechanism. Since the  
645 experiment were done at low RH the direct hydrolysis would be less likely (see Rindelaub et al.  
646 2015, 2016). However, knowing HNO<sub>3</sub> being thermodynamic stable one may speculate in that  
647 dimerization of two monomer species via the loss of one HNO<sub>3</sub> molecule could occur e.g. where  
648 a C<sub>20</sub>H<sub>29</sub>NO<sub>y</sub> (y = 10–18) species would be generated from C<sub>10</sub>H<sub>15</sub>NO<sub>x</sub> (x = 5–9) species. This  
649 process could be seen as the reverse of esterification in order to produce a dimer product with one  
650 less nitrogen and reduced numbers of oxygens. For example, with HNO<sub>3</sub> as a leaving group, the  
651 mechanism of dimerization between C<sub>10</sub>H<sub>15</sub>NO<sub>6</sub> and C<sub>10</sub>H<sub>15</sub>NO<sub>8</sub> (see Reaction 3), would produce  
652 the C<sub>20</sub> dimer species (C<sub>20</sub>H<sub>29</sub>NO<sub>11</sub>) that was observed in all experiments. The formation of the  
653 observed C<sub>19</sub> dimer species (e.g., C<sub>19</sub>H<sub>27</sub>O<sub>15</sub>) through the combination of, for example,  
654 C<sub>10</sub>H<sub>17</sub>NO<sub>7</sub> and C<sub>9</sub>H<sub>11</sub>NO<sub>11</sub> monomer species (Reaction 4) is also attributed to this mechanism.  
655 Additionally, the occurrence of dimer species with two nitrogen atoms, through the combination  
656 of monomers such as C<sub>10</sub>H<sub>16</sub>N<sub>2</sub>O<sub>9</sub> and C<sub>9</sub>H<sub>13</sub>NO<sub>8</sub> (Reaction 5), can also be attributed to this  
657 dimerization mechanism.



661 The higher O/C ratios of the monomer species, compared with those of the  
662 dimers/oligomers, may also be attributed to the loss of an HNO<sub>3</sub> molecule (from the monomer)  
663 during the dimerization process. For example, the two C<sub>10</sub> reactants in Reaction 3 have O/C ratios  
664 of 0.6 and 0.8 while the product, C<sub>20</sub>H<sub>29</sub>NO<sub>11</sub>, has an O/C ratio of 0.55. A similar trend is  
665 observed for Reactions 4 and 5, where the reactants have an average O/C ratio of 0.96 and 0.89,

Deleted: correlation

Deleted: average O/C ratios

Deleted: (

Deleted: (clusters 3 and 4) groupings, with more highly oxygenated species desorbing at higher temperatures than their less-oxygenated counterparts. This is also reflected in the overall oxidation state of the clusters (2×O/C - H/C - 5×N/C). However, this trend is observed for only a certain range of masses, as lower MW

Deleted: This

Deleted: Based on the behavior observed in the thermograms for species measured from the limonene SOA in this study, a

Deleted: of dimer formation,

Deleted: occurring in

Deleted: particle phase, can

Deleted: proposed. Dimerization

Deleted: may

Deleted: during the processes, and

687 respectively, and the products have O/C ratios of 0.79 and 0.74, respectively. Due to the loss of  
688 HNO<sub>3</sub> during dimerization, the potential dimer decomposition during desorption is expected to  
689 yield fragments which differ in molecular composition from the precursor (i.e., pre-dimerization)  
690 monomers. However, the resulting monomers may also be associated with aerosol phase products  
691 that have secondary desorption peaks. For example, the fragmentation of C<sub>20</sub>H<sub>29</sub>NO<sub>11</sub> could yield  
692 C<sub>10</sub>H<sub>14</sub>O<sub>6</sub> + C<sub>10</sub>H<sub>15</sub>NO<sub>5</sub> or C<sub>10</sub>H<sub>16</sub>O<sub>5</sub> + C<sub>10</sub>H<sub>13</sub>NO<sub>6</sub>, and the fragmentation of C<sub>19</sub>H<sub>27</sub>NO<sub>15</sub> might  
693 yield C<sub>9</sub>H<sub>13</sub>NO<sub>6</sub> + C<sub>10</sub>H<sub>14</sub>O<sub>9</sub> or C<sub>9</sub>H<sub>13</sub>NO<sub>9</sub> + C<sub>10</sub>H<sub>14</sub>O<sub>6</sub>. Likewise, C<sub>9</sub>H<sub>13</sub>NO<sub>7</sub> + C<sub>10</sub>H<sub>15</sub>NO<sub>7</sub> or  
694 C<sub>9</sub>H<sub>13</sub>NO<sub>9</sub> + C<sub>10</sub>H<sub>15</sub>NO<sub>5</sub> monomer pairs could be generated from the thermal degradation of  
695 C<sub>19</sub>H<sub>28</sub>N<sub>2</sub>O<sub>14</sub>.

Deleted: fragmentation

Deleted: monomers

Deleted: original

696 The fragmentation of dimers may also proceed through multiple channels, thereby  
697 producing several sets of monomer fragments, or the fragmentation of multiple dimers may  
698 produce the same ions. Therefore, attributing the production of a monomer fragment to the  
699 thermal degradation of a specific dimer is difficult, using the current dataset. Large (C > 20)  
700 oligomeric species may contribute to the high-temperature generation of monomer fragment  
701 species. The proposed mechanisms may play only a partial role in the dimerization process  
702 occurring in these experiments. However, they offer a plausible explanation for the occurrence of  
703 multiple observed dimers and the secondary desorption maxima associated with the monomer  
704 constituents.

#### 705 4 Conclusions

706 High-resolution mass spectrometric data was analysed for condensed-phase reaction  
707 products resulting from NO<sub>3</sub> initiated oxidation of the monoterpene, limonene. The results  
708 revealed that the formation of organic nitrates contributed substantially (89.5 ± 1.4% of the  
709 particulate-phase ion signal) to SOA formation, with dimers constituting a significant fraction of  
710 the particle-phase products. On average, monomers and dimers/oligomers contributed 63 ± 7, and  
711 37 ± 7%, respectively, of the particle-phase organic signal detected by the I-CIMS. Furthermore,  
712 many monomers (accounting for 22 ± 3% of the average organic signal) desorbed at high  
713 temperatures (120°C). The fraction of the signal generated by monomers increased with  
714 increasing N<sub>2</sub>O<sub>5</sub>/limonene ratio (ratio of 43 yields a fraction of 76%), whereas the fraction of  
715 dimers decreased (to 24%). The fraction of the monomer signal resulting from desorption at high  
716 temperatures (≥120°C) also increased (by 26%). Therefore, although the monomer fraction  
717 increased with increasing N<sub>2</sub>O<sub>5</sub>/limonene ratio, this increase in desorption signal occurred  
718 primarily at temperatures above 120°C, indicative of an increase in the fragmentation of high-  
719 MW dimers and oligomers. A large portion (79%) of the monomer thermograms exhibited this  
720 bi-modal behavior, with secondary peaks occurring above 120°C, indicating that the composition  
721 of SOA was largely determined by the formation of thermally unstable, low-volatility oligomers.

Deleted: obtained

Deleted: both gas and

Deleted: 62.6

Deleted: .2

Deleted: .4

Deleted: .3

Deleted: 21.6

Deleted: .1

Deleted: 42.5

Deleted: 75.8

Deleted: .2

Deleted: .2

722 In total, 196 individual organic ions were detected during desorption. However, the total  
723 measured organic signal was generated mainly by 52 (i.e., 76%) of these ions, which constituted  
724 the 75<sup>th</sup> percentile of the monomer and dimer signals. Over half of the signal emanated from the



740 top 90<sup>th</sup> percentile, which comprised a small subset of only 20 species, of the total number of  
741 ions. These 20 species (with nine listed as major products in the MCM) constituted the major  
742 particle-phase products formed via the reaction of N<sub>2</sub>O<sub>5</sub> and limonene under the conditions  
743 employed in this study. The non-listed species (see Table S1) were either dimer species or more  
744 highly oxygenated, nitrated analogs of known major products, which are notoriously hard to  
745 describe via standard gas-phase mechanisms. There are two frequently suggested pathways for  
746 these. Firstly, the high number of oxygens would be result of isomerization of RO or RO<sub>2</sub> that  
747 rarely is described explicit in current modelling framework. Secondly, the presence of di-nitrated  
748 compounds relies on secondary chemistry derived from e.g. produced mononitrates  
749 intermediates; for limonene containing two double bonds this is more relevant than for other  
750 monoterpenes and so far not commonly described in models.

751 Cluster analysis revealed two monomer groups, two dimer groups and, a separate group  
752 containing monomer ions that exhibited secondary desorption peaks occurring at temperatures  
753  $\geq 150^{\circ}\text{C}$ . Each group was characterized by a distinct average MW and desorption temperature  
754 ( $T_{\text{max}}$ ). The 2 identified clusters in the monomer and dimer sub-classes differ in oxidation state  
755 and O/C ratios, with increasing O/C corresponding to higher  $T_{\text{max}}$  values.

756 Using a combination of cluster analysis and thermal properties derived from FIGAERO-  
757 CIMS measurements may provide some means of reducing the complexity associated with the  
758 description of SOA formation processes. The investigated reaction system constitutes only one of  
759 many systems, but could be used as an example of the evaluation required for this type of  
760 information derived from high-resolution MS. The results revealed that, analogous to products  
761 from ozonolysis and  $\cdot\text{OH}$ -induced oxidation, the organic nitrates produced in the nighttime  
762 chemistry of biogenic compounds comprise a multi-component mixture that contributes to  
763 ambient SOA. Thus, the aerosol species detected here could be included in modeling studies with  
764 the aim of explaining scenarios where SOA formation rates are under-predicted. Furthermore, the  
765 numerous products resulting from  $\text{NO}_3$  oxidation of limonene, which were identified and grouped  
766 based on thermal properties, could be candidates for identification in ambient air masses  
767 dominated by nocturnal limonene chemistry.

## 768 Competing interests

769 The authors declare that they have no conflict of interest.

770

## 771 Acknowledgment

772 The research presented is a contribution to the Swedish strategic research area Modelling the  
773 Regional and Global Earth system, MERGE. This work was supported by the Swedish Research  
774 Council (grant numbers 2015-04123; 2014-05332; 2013-06917), Formas (grant number 2015-  
775 1537)

Deleted: Based on the analysis of these monomer and dimer groups, a mechanism (Reactions 3–5) was proposed for the formation of the observed dimers from the monomers.

Deleted: Figaero

Deleted: N<sub>2</sub>O<sub>5</sub>

783 **References**

- 784 Arthur, D. and Vassilvitskii, S.: k-means ++: The advantages of careful seeding, ACM-SIAM  
785 Symp. Discret. algorithms, 8, 1027–1035, doi:10.1145/1283383.1283494, 2007.
- 786 Atkinson, R., Aschmann, S. M., and Pitts, J. N. J.: Rate constants for the gas-phase reactions of  
787 the OH radical with a series of monoterpenes at 294 K, Atmos. Environ., 29(17), 2311–2316
- 788 Ayres, B. R., Allen, H. M., Draper, D. C., Brown, S. S., Wild, R. J., Jimenez, J. L., Day, D. A.,  
789 Campuzano-Jost, P., Hu, W., de Gouw, J., Koss, A., Cohen, R. C., Duffey, K. C., Romer, P.,  
790 Baumann, K., Edgerton, E., Takahama, S., Thornton, J. A., Lee, B. H., Lopez-Hilfiker, F. D.,  
791 Mohr, C., Goldstein, A. H., Olson, K., and Fry, J. L.: Organic nitrate aerosol formation via NO<sub>3</sub>  
792 + BVOC in the Southeastern US, Atmos. Chem. Phys. Discuss., 15(12), 16235–16272,  
793 doi:10.5194/acpd-15-16235-2015, 2015.
- 794 Baptista, L., Pfeifer, R., Da Silva, E. C. and Arbilla, G.: Kinetics and thermodynamics of  
795 limonene ozonolysis, J. Phys. Chem. A, 115(40), 10911–10919, doi:10.1021/jp205734h, 2011.
- 796 Beaver, M. R., Clair, J. M. St., Paulot, F., Spencer, K. M., Crounse, J. D., LaFranchi, B. W., Min,  
797 K. E., Pusede, S. E., Wooldridge, P. J., Schade, G. W., Park, C., Cohen, R. C., and Wennberg, P.  
798 O.: Importance of biogenic precursors to the budget of organic nitrates: Observations of  
799 multifunctional organic nitrates by CIMS and TD-LIF during BEARPEX 2009, Atmos. Chem.  
800 Phys., 12(13), 5773–5785, doi:10.5194/acp-12-5773-2012, 2012.
- 801 Bonn, B. and Moorgat, G. K.: New particle formation during  $\alpha$ - and  $\beta$ -pinene oxidation by O<sub>3</sub>,  
802 OH and NO<sub>3</sub>, and the influence of water vapour: Particle size distribution studies, Atmos. Chem.  
803 Phys., 2, 183–196, doi:doi:10.5194/acp-2-183-2002, 2002.
- 804 [Boyd, C. M., Nah, T., Xu, L., Berkemeir, T., and Lee Ng, N.: Secondary Organic Aerosol \(SOA\)  
805 from nitrate radical oxidation of monoterpenes: Effects of temperature, dilution and humidity on  
806 aerosol formations, mixing, and evaporation, Environ. Sci. Technol., 51, 14, 7831-7841, 2017.](#)
- 807 Brown, S. S. and Stutz, J.: Nighttime radical observations and chemistry, Chem. Soc. Rev.,  
808 41(19), 6405, doi:10.1039/c2cs35181a, 2012.
- 809 Bruns, E. A, Perraud, V., Zelenyuk, A., Ezell, M. J., Johnson, S. N., Yu, Y., Imre, D., Finlayson-  
810 Pitts, B. J., and Alexander, M. L.: Comparison of FTIR and particle mass spectrometry for the  
811 measurement of particulate organic nitrates., Environ. Sci. Technol., 44(3), 1056–1061,  
812 doi:10.1021/es9029864, 2010.
- 813 Cao, G. and Jang, M.: Secondary organic aerosol formation from toluene photooxidation under  
814 various NO<sub>x</sub> conditions and particle acidity, Atmos. Chem. Phys. Discuss., 8(4), 14467–14495,  
815 doi:10.5194/acpd-8-14467-2008, 2008.
- 816 [Carlton, A. G., Wiedinmyer, C., and Kroll, J. H.: A review of secondary organic aerosol \(SOA\)  
817 formation from isoprene, Atmos. Chem. Phys. Discuss., 9\(2\), 8261–8305, doi:10.5194/acpd-9-  
818 8261-2009, 2009.](#)

Moved (insertion) [1]

Moved (insertion) [2]

Deleted: — Page Break —

821 [Day, D. A., Liu, S., Russell, L. M., and Ziemann, P. J.: Organonitrate group concentrations in](#)  
822 [submicron particles with high nitrate and organic fractions in coastal southern California, \*Atmos.\*](#)  
823 [Environ., 44, 1970–1979, 2010.](#)

Moved (insertion) [3]

Moved (insertion) [4]

Moved (insertion) [5]

824 Donahue, N. M., Kroll, J. H., Pandis, S. N., and Robinson, A. L.: A two-dimensional volatility  
825 basis set-Part 2: Diagnostics of organic-aerosol evolution, *Atmos. Chem. Phys.*, 12(2), 615–634,  
826 doi:10.5194/acp-12-615-2012, 2012.

827 Ehn, M., Thornton, J. A., Kleist, E., Sipilä, M., Junninen, H., Pullinen, I., Springer, M., Rubach,  
828 F., Tillmann, R., Lee, B., Lopez-Hilfiker, F., Andres, S., Acir, I.-H., Rissanen, M., Jokinen, T.,  
829 Schobesberger, S., Kangasluoma, J., Kontkanen, J., Nieminen, T., Kurtén, T., Nielsen, L. B.,  
830 Jørgensen, S., Kjaergaard, H. G., Canagaratna, M., Maso, M. D., Berndt, T., Petäjä, T., Wahner,  
831 A., Kerminen, V.-M., Kulmala, M., Worsnop, D. R., Wildt, J., and Mentel, T. F.: A large source  
832 of low-volatility secondary organic aerosol, *Nature*, 506(7489), 476–479,  
833 doi:10.1038/nature13032, 2014.

834 Emanuelsson, E. U., Hallquist, M., Kristensen, K., Glasius, M., Bohn, B., Fuchs, H., Kammer,  
835 B., Kiendler-Scharr, A., Nehr, S., Rubach, F., Tillmann, R., Wahner, A., Wu, H. C., and Mentel,  
836 T. F.: Formation of anthropogenic secondary organic aerosol (SOA) and its influence on biogenic  
837 SOA properties, *Atmos. Chem. Phys.*, 13(5), 2837–2855, doi:10.5194/acp-13-2837-2013, 2013.

838 Fry, J. L., Draper, D. C., Barsanti, K. C., Smith, J. N., Ortega, J., Winkler, P. M., Lawler, M. J.,  
839 Brown, S. S., Edwards, P. M., Cohen, R. C., and Lee, L.: Secondary organic aerosol formation  
840 and organic nitrate yield from NO<sub>3</sub> oxidation of biogenic hydrocarbons, *Environ. Sci. Technol.*,  
841 48(3), 11944–11953

842 Fry, J. L., Kiendler-Scharr, A., Rollins, A. W., Brauers, T., Brown, S. S., Dorn, H.-P., Dubé, W.  
843 P., Fuchs, H., Mensah, A., Rohrer, F., Tillmann, R., Wahner, A., Wooldridge, P. J., and Cohen,  
844 R. C.: SOA from limonene: role of NO<sub>3</sub> in its generation and degradation, *Atmos. Chem. Phys.*,  
845 11(8), 3879–3894, doi:10.5194/acp-11-3879-2011, 2011.

846 Fry, J. L., Rollins, A. W., Wooldridge, P. J., Brown, S. S., Fuchs, H., and Dub, W.: Organic  
847 nitrate and secondary organic aerosol yield from NO<sub>3</sub> oxidation of β-pinene evaluated using a  
848 gas-phase kinetics / aerosol partitioning model, *Atmos. Chem. Phys.*, 9(3), 1431–1449,  
849 doi:10.5194/acp-9-1431-2009, 2009.

850 Glasius, M. and Goldstein, A. H.: Recent discoveries and future challenges in atmospheric  
851 organic chemistry, *Environ. Sci. Technol.*, 50(6), 2754–2764, doi:10.1021/acs.est.5b05105, 2016.

852 Guenther, A. B., Jiang, X., Heald, C. L., Sakulyanontvittaya, T., Duhl, T., Emmons, L. K., and  
853 Wang, X.: The model of emissions of gases and aerosols from nature version 2.1 (MEGAN2.1):  
854 An extended and updated framework for modeling biogenic emissions, *Geosci. Model Dev.*, 5(6),  
855 1471–1492, doi:10.5194/gmd-5-1471-2012, 2012.

856 Guenther, A., Karl, T., Harley, P., Wiedinmyer, C., Palmer, P. I., and Geron, C.: Estimates of  
857 global terrestrial isoprene emissions using MEGAN (Model of Emissions of Gases and Aerosols  
858 from Nature), *Atmos. Chem. Phys.*, 6(11), 3181–3210, doi:10.5194/acpd-6-107-2006, 2006.

859 [Guenther, A., Nicholas, C., Erickson, D., Fall, R., Geron, C., Graedel, T., Harley, P., Klinger, L.,](#)

Deleted: -----Page Break-----

¶

- 862 Lerda, M., McKay, W. A., Pierce, T., Scholes, B., Steinbrecher, R., Tallamraju, R., Taylor, J.,  
863 and Zimmerman, P.: A global model of natural volatile organic compound emissions, *J. Geophys.*  
864 *Res.*, 100(94), 8873–8892
- 865 Hallquist, M., Wängberg, I., Ljungström, E., Barnes, I., and Becker, K. H.: Aerosol and product  
866 yields from NO<sub>3</sub> radical-initiated oxidation of selected monoterpenes, *Environ. Sci. Technol.*,  
867 33(4), 553–559, doi:10.1021/es980292s, 1999.
- 868 Hallquist, M., Wenger, J. C., Baltensperger, U., Rudich, Y., Simpson, D., Claeys, M., Dommen,  
869 J., Donahue, N. M., George, C., Goldstein, A. H., Hamilton, J. F., Herrmann, H., Hoffmann, T.,  
870 Iinuma, Y., Jang, M., Jenkin, M. E., Jimenez, J. L., Kiendler-Scharr, A., Maenhaut, W.,  
871 McFiggans, G., Mentel, T. F., Monod, A., Prévôt, A. S. H., Seinfeld, J. H., Surratt, J. D.,  
872 Szmigielski, R., and Wildt, J.: The formation, properties and impact of secondary organic  
873 aerosol: current and emerging issues, *Atmos. Chem. Phys.*, 9(14), 5155–5236, doi:10.5194/acp-9-  
874 5155-2009, 2009.
- 875 Holzinger, R., Kasper-Giebl, A., Staudinger, M., Schauer, G., and Röckmann, T.: Analysis of the  
876 chemical composition of organic aerosol at the Mt. Sonnblick observatory using a novel high  
877 mass resolution thermal-desorption proton-transfer-reaction mass-spectrometer (HR-TD-PTR-  
878 MS), *Atmos. Chem. Phys.*, 10(20), 10111–10128, doi:10.5194/acp-10-10111-2010, 2010.
- 879 Jiang, L., Lan, R., Xu, Y. S., Zhang, W. J., and Yang, W.: Reaction of stabilized criegee  
880 intermediates from ozonolysis of limonene with water: Ab initio and DFT study, *Int. J. Mol. Sci.*,  
881 14(3), 5784–5805, doi:10.3390/ijms14035784, 2013.
- 882 Jimenez, J. L., Canagaratna, M. R., Donahue, N. M., Prevot, A. S. H., Zhang, Q., Kroll, J. H.,  
883 Decarlo, P. F., Allan, J. D., Coe, H., Ng, N. L., Aiken, A. C., Ulbrich, I. M., Grieshop, A. P.,  
884 Duplissy, J., Wilson, K. R., Lanz, V. A., Hueglin, C., Sun, Y. L., Tian, J., Laaksonen, A.,  
885 Raatikainen, T., Rautiainen, J., Vaattovaara, P., Ehn, M., Kulmala, M., Tomlinson, J. M.,  
886 Cubison, M. J., Dunlea, E. J., Alfarra, M. R., Williams, P. I., Bower, K., Kondo, Y., Schneider,  
887 J., Drewnick, F., Borrmann, S., Weimer, S., Demerjian, K., Salcedo, D., Cottrell, L., Takami, A.,  
888 Miyoshi, T., Shimojo, A., Sun, J. Y., Zhang, Y. M., Dzepina, K., Sueper, D., Jayne, J. T.,  
889 Herndon, S. C., Williams, L. R., Wood, E. C., Middlebrook, A. M., Kolb, C. E., Baltensperger,  
890 U., and Worsnop, D. R.: Evolution of organic aerosols in the atmosphere, *Science* 326, 1525–  
891 1529
- 892 Jokinen, T., Berndt, T., Makkonen, R., Kerminen, V.-M., Junninen, H., Paasonen, P., Stratmann,  
893 F., Herrmann, H., Guenther, A. B., Worsnop, D. R., Kulmala, M., Ehn, M., and Sipilä, M.:  
894 Production of extremely low volatile organic compounds from biogenic emissions: Measured  
895 yields and atmospheric implications., *Proc. Natl. Acad. Sci. U. S. A.*, 112(23), 7123–7128,  
896 doi:10.1073/pnas.1423977112, 2015.
- 897 Jonsson, Å. M., Hallquist, M., and Ljungström, E.: Impact of humidity on the ozone initiated  
898 oxidation of limonene,  $\Delta^3$ -carene, and  $\alpha$ -pinene, *Environ. Sci. Technol.*, 40(1), 188–194,  
899 doi:10.1021/es051163w, 2006.
- 900 | Jonsson, Å. M., Hallquist, M., and Ljungström, E.: The effect of temperature and water on  
901 secondary organic aerosol formation from ozonolysis of limonene,  $\Delta^3$ -carene and  $\alpha$ -pinene,  
902 *Atmos. Chem. Phys.*, 8(21), 6541–6549, doi:10.5194/acp-8-6541-2008, 2008a.

905 Jonsson, Å. S. A. M., Hallquist, M., Ljungstro, E., Jonsson, Å. S. A. M., and Hallquist, M.:  
906 Influence of OH scavenger on the water effect on secondary organic influence of OH scavenger  
907 on the water effect on secondary organic aerosol formation from ozonolysis of limonene,  $\Delta^3$ -  
908 carene, and  $\alpha$ -pinene, *Environ. Sci. Technol.*, 42(16), 5938–5944, doi:10.1021/es702508y, 2008b.

909 Kanakidou, M., Seinfeld, J. H., Pandis, S. N., Barnes, I., Dentener, F. J., Facchini, M. C., Van  
910 Dingenen, R., Ervens, B., Nenes, A., Nielsen, C. J., Swietlicki, E., Putaud, J. P., Balkanski, Y.,  
911 Fuzzi, S., Horth, J., Moortgat, G. K., Winterhalter, R., Myhre, C. E. L., Tsigaridis, K., Vignati,  
912 E., Stephanou, E. G., and Wilson, J.: Organic aerosol and global climate modelling: A review,  
913 *Atmos. Chem. Phys.*, 5(4), 1053–1123, doi:10.5194/acp-5-1053-2005, 2005.

914 Kiendler-Scharr, A., Mensah, A. A., Friese, E., Topping, D., Nemitz, E., Prevot, A. S. H., Äijälä, M., Allan,  
915 J., Canonaco, F., Canagaratna, M., Carbone, S., Crippa, M., Dall'Osto, M., Day, D. A., De Carlo, P., Di  
916 Marco, C. F., Elbern, H., Eriksson, A., Freney, E., Hao, J., Herrmann, H., Hildebrandt, L., Hillamo, R.,  
917 Jimenez, J. L., Laaksonen, A., McFiggans, G., Mohr, C., O'Dowd, C., Otjes, R., Ovadnevaite, J., Pandis, S. N.,  
918 Poulain, L., Schlag, P., Sellegri, K., Swietlicki, E., Tiitta, P., Vermeulen, A., Wahner, A., Worsnop, D., and  
919 Wu, H. C.: Ubiquity of organic nitrates from nighttime chemistry in the European submicron aerosol,  
920 *Geophys. Res. Lett.*, 43, 7735–7744, 10.1002/2016GL069239, 2016

921 Kourtchev, I., Fuller, S. J., Giorio, C., Healy, R. M., Wilson, E., O'Connor, I., Wenger, J. C.,  
922 McLeod, M., Aalto, J., Ruuskanen, T. M., Maenhaut, W., Jones, R., Venables, D. S., Sodeau, J.  
923 R., Kulmala, M., and Kalberer, M.: Molecular composition of biogenic secondary organic  
924 aerosols using ultrahigh-resolution mass spectrometry: Comparing laboratory and field studies,  
925 *Atmos. Chem. Phys.*, 14(4), 2155–2167, doi:10.5194/acp-14-2155-2014, 2014.

926 Kourtchev, I., Giorio, C., Manninen, A., Wilson, E., Mahon, B., Aalto, J., Kajos, M., Venables,  
927 D., Ruuskanen, T., Levula, J., Loponen, M., Connors, S., Harris, N., Zhao, D., Kiendler-Scharr,  
928 A., Mentel, T., Rudich, Y., Hallquist, M., Doussin, J.-F., Maenhaut, W., Bäck, J., Petäjä, T.,  
929 Wenger, J., Kulmala, M., and Kalberer, M.: Enhanced Volatile Organic Compounds emissions  
930 and organic aerosol mass increase the oligomer content of atmospheric aerosols, *Nat. Sci.*  
931 *Reports*, 6(September), 35038, doi:10.1038/srep35038, 2016.

932 Kristensen, K., Watne, Å. K., Hammes, J., Lutz, A., Petäjä, T., Hallquist, M., Bilde, M., and  
933 Glasius, M.: High-molecular weight dimer esters are major products in aerosols from  $\alpha$ -pinene  
934 ozonolysis and the Boreal forest, *Environ. Sci. Technol. Lett.*, 3(8), 280–285,  
935 doi:10.1021/acs.estlett.6b00152, 2016.

936 Kroll, J. H., Chan, A. W. H., Ng, N. G. A. L., and Flagan, R. C.: Reactions of semivolatile  
937 organics and their Effects on secondary organic aerosol formation, *Environ. Sci. Technol.*,  
938 41(10), 3545–3550

939 Kroll, J. H. and Seinfeld, J. H.: Chemistry of secondary organic aerosol: Formation and evolution  
940 of low-volatility organics in the atmosphere, *Atmos. Environ.*, 42(16), 3593–3624,  
941 doi:10.1016/j.atmosenv.2008.01.003, 2008.

942 Lee, B. H., Lopez-Hilfiker, F. D., Mohr, C., Kurtén, T., Worsnop, D. R., and Thornton, J. A.: An  
943 iodide-adduct high-resolution time-of-flight chemical-ionization mass spectrometer: Application  
944 to atmospheric inorganic and organic compounds., *Environ. Sci. Technol.*, 48(11), 6309–6317,  
945 doi:10.1021/es500362a, 2014a.

Moved (insertion) [6]

Moved (insertion) [7]

Moved (insertion) [8]

Moved (insertion) [9]

Moved (insertion) [10]

Moved (insertion) [11]

Moved (insertion) [12]

946 | Lee, B. H., Mohr, C., Lopez-Hilfiker, F. D., Lutz, A., Hallquist, M., Lee, L., Romer, P., Cohen,  
947 R. C., Iyer, S., Kurten, T., Hu, W., Day, D. A., Campuzano-Jost, P., Jimenez, J. L., Xu, L., Ng, N.  
948 L., Guo, H., Weber, R. J., Wild, R. J., Brown, S. S., Koss, A., de Gouw, J., Olson, K., Goldstein,  
949 A. H., Seco, R., Kim, S., McAvey, K., Shepson, P. B., Starn, T., Baumann, K., Edgerton, E. S.,  
950 Liu, J., Shilling, J. E., Miller, D. O., Brune, W., Schobesberger, S., D'Ambro, E. L., and  
951 Thornton, J. A.: Highly functionalized organic nitrates in the southeast United States:  
952 Contribution to secondary organic aerosol and reactive nitrogen budgets, *Proc. Natl. Acad. Sci.*  
953 *U. S. A.*, 113(6), 1516–1521, doi:10.1073/pnas.1508108113, 2016.

954 Lee, L., Wooldridge, P. J., Gilman, J. B., Warneke, C., de Gouw, J., and Cohen, R. C.: Low  
955 temperatures enhance organic nitrate formation: Evidence from observations in the 2012 Uintah  
956 Basin Winter Ozone Study, *Atmos. Chem. Phys.*, 14(22), 12441–12454, doi:10.5194/acp-14-  
957 12441-2014, 2014b.

958 Leungsakul, S., Jaoui, M., and Kamens, R. M.: Kinetic mechanism for predicting secondary  
959 organic aerosol formation from the reaction of d-limonene with ozone., *Environ. Sci. Technol.*,  
960 39(24), 9583–9594, doi:10.1021/es0492687, 2005.

961 Lopez-Hilfiker, F. D., Mohr, C., Ehn, M., Rubach, F., Kleist, E., Wildt, J., Mentel, T. F.,  
962 Carrasquillo, A., Daumit, K., Hunter, J., Kroll, J. H., Worsnop, D., and Thornton, J. A.: Phase  
963 partitioning and volatility of secondary organic aerosol components formed from  $\alpha$ -pinene  
964 ozonolysis and OH oxidation: The importance of accretion products and other low volatility  
965 compounds, *Atmos. Chem. Phys. Discuss.*, 15, 4463–4494, doi:10.5194/acpd-15-4463-2015,  
966 2015.

967 Lopez-Hilfiker, F. D., Mohr, C., Ehn, M., Rubach, F., Kleist, E., Wildt, J., Mentel, T. F., Lutz,  
968 A., Hallquist, M., Worsnop, D., and Thornton, J. A.: A novel method for online analysis of gas  
969 and particle composition: Description and evaluation of a Filter Inlet for Gases and AEROSols  
970 (FIGAERO), *Atmos. Meas. Tech.*, 7(4), 983–1001, doi:DOI 10.5194/amt-7-983-2014, 2014.

971 McKinney, W.: Data structures for statistical computing in Python, *Proc. 9th Python Sci. Conf.*,  
972 1697900(Scipy), 51–56 [online] Available from:  
973 <http://conference.scipy.org/proceedings/scipy2010/mckinney.html>, 2010.

974 McKinney, W.: pandas: A foundational Python library for data analysis and statistics, *Python*  
975 *High Perform. Sci. Comput.*, 1–9

976 Mentel, T. F., Springer, M., Ehn, M., Kleist, E., Pullinen, I., Kurtén, T., Rissanen, M., Wahner,  
977 A., and Wildt, J.: Formation of highly oxidized multifunctional compounds: Autoxidation of  
978 peroxy radicals formed in the ozonolysis of alkenes – deduced from structure–product  
979 relationships, *Atmos. Chem. Phys.*, 15(12), 6745–6765, doi:10.5194/acp-15-6745-2015, 2015.

980 Müller, L., Reinnig, M.-C., Warnke, J., and Hoffmann, T.: Unambiguous identification of esters  
981 as oligomers in secondary organic aerosol formed from cyclohexene and cyclohexene/ $\alpha$ -pinene  
982 ozonolysis, *Atmos. Chem. Phys. Discuss.*, 7, 13883–13913, doi:10.5194/acpd-7-13883-2007,  
983 2007.

984 | Murphy, B. N., Donahue, N. M., Robinson, A. L., and Pandis, S. N.: A naming convention for  
985 atmospheric organic aerosol, *Atmos. Chem. Phys.*, 14(11), 5825–5839, doi:10.5194/acp-14-5825-

Deleted: —Page Break—  
¶

Deleted: —Page Break—  
¶



990 2014, 2014.

991 Myhre, G., Shindell, D., Bréon, F.-M., Collins, W., Fuglestedt, J., Huang, J., Koch, D.,  
992 Lamarque, J.-F., Lee, D., Mendoza, B., Nakajima, T., Robock, A., Stephens, G., Takemura, T.,  
993 and Zhan, H.: Anthropogenic and natural radiative forcing: In Climate Change 2013: The  
994 Physical Science Basis. Contribution of Working Group I to the Fifth Assessment Report of the  
995 Intergovernmental Panel on Climate Change, Cambridge Univ. Press. Cambridge, United  
996 Kingdom New York, NY, USA, 659–740, doi:10.1017/ CBO9781107415324.018, 2013.

997 [Nah, T., McVay, R. C., Zhang, X., Boyd, C. M., Seinfeld, J. H., and Ng, N. L.: Influence of seed](#)  
998 [aerosol surface area and oxidation rate on vapor wall deposition and SOA mass yields: a case](#)  
999 [study with  \$\alpha\$ -pinene ozonolysis, Atmos. Chem. Phys., 16, 9361-9379, 10.5194/acp-16- 210 9361-](#)  
1000 [2016, 2016.](#)

1001 [Ng, N. L., Brown, S. S., Archibald, A. T., Atlas, E., Cohen, R. C., Crowley, J. N., Day, D. A.,](#)  
1002 [Donahue, N. M., Fry, J. L., Fuchs, H., Griffin, R. J., Guzman, M. I., Herrmann, H., Hodzic, A.,](#)  
1003 [Iinuma, Y., Jimenez, J. L., Kiendler-Scharr, A., Lee, B. H., Luecken, D. J., Mao, J., McLaren, R.,](#)  
1004 [Mutzel, A., Osthoff, H. D., Ouyang, B., Picquet-Varrault, B., Platt, U., Pye, H. O. T., Rudich, Y.,](#)  
1005 [Schwantes, R. H., Shiraiwa, M., Stutz, J., Thornton, J. A., Tilgner, A., Williams, B. J., and](#)  
1006 [Zaveri, R. A.: Nitrate radicals and biogenic volatile organic compounds: oxidation, mechanisms,](#)  
1007 [and organic aerosol, Atmos. Chem. Phys., 17, 2103–2162, https://doi.org/10.5194/acp-17-2103-](#)  
1008 [2017, 2017.](#)

1009 Pathak, R. K., Salo, K., Emanuelsson, E. U., Cai, C., Lutz, A., Hallquist, Å. M., and Hallquist,  
1010 M.: Influence of ozone and radical chemistry on limonene organic aerosol production and  
1011 thermal characteristics, Environ. Sci. Technol., 46, 11660–11669

1012 Paulot, F., Crounse, J. D., Kjaergaard, H. G., Kroll, J. H., Seinfeld, J. H., and Wennberg, P. O.:  
1013 Isoprene photooxidation: New insights into the production of acids and organic nitrates, Atmos.  
1014 Chem. Phys., 9(4), 1479–1501, doi:10.5194/acp-9-1479-2009, 2009.

1015 Pedregosa, F., Grisel, O., Weiss, R., Passos, A., and Brucher, M.: Scikit-learn: Machine learning  
1016 in Python, J. Mach. Learn. Res., 12, 2825–2830, doi:10.1007/s13398-014-0173-7.2, 2011.

1017 Perraud, V., Bruns, E. A., Ezell, M. J., Johnson, S. N., Greaves, J., and Finlayson-Pitts, B. J.:  
1018 Identification of organic nitrates in the NO<sub>3</sub> radical initiated oxidation of alpha-pinene by  
1019 atmospheric pressure chemical ionization mass spectrometry., Environ. Sci. Technol., 44(15),  
1020 5887–93, doi:10.1021/es1005658, 2010.

1021 Perring, A. E., Bertram, T. H., Wooldridge, P. J., Fried, A., Heikes, B. G., Dibb, J., Crounse, J.  
1022 D., Wennberg, P. O., Blake, N. J., Blake, D. R., Brune, W. H., Singh, H. B., and Cohen, R. C.:  
1023 Airborne observations of total RONO<sub>2</sub>: New constraints on the yield and lifetime of isoprene  
1024 nitrates, Atmos. Chem. Phys., 9(4), 1451–1463, doi:10.5194/acp-9-1451-2009, 2009.

1025 Perring, A. E., Pusede, S. E., and Cohen, R. C.: An observational perspective on the atmospheric  
1026 impacts of alkyl and multifunctional nitrates on ozone and secondary organic aerosol, Chem.  
1027 Rev.

1028 Presto, A. A., Hartz, K. E. H., and Donahue, N. M.: Secondary organic aerosol production from

Moved up [10]: J.,

Deleted: Orlando, J.

Moved up [3]: S.,

Moved up [2]: Environ.

Deleted: Tyndall, G.

Deleted: and Calvert, J. G.: Thermal decomposition pathways for peroxyacetyl nitrate (PAN): Implications for atmospheric methyl nitrate levels, Atmos.

Moved (insertion) [13]

Deleted: Part A, Gen. Top., 26(17), 3111–3118, doi:10.1016/0960-1686(92)90468-Z, 1992.¶



1041 terpene ozonolysis. 1. Effect of UV radiation., Environ. Sci. Technol., 39(18), 7036–7045,  
1042 doi:10.1021/es050174m, 2005a.

1043 Presto, A. A., Hartz, K. E. H., Donahue, N. M., Huff Hartz, K. E., Donahue, N. M., Hartz, K. E.  
1044 H., Donahue, N. M., Huff Hartz, K. E., and Donahue, N. M.: Secondary organic aerosol  
1045 production from terpene ozonolysis. 2. Effect of NO<sub>x</sub> concentration, Environ. Sci. Technol.,  
1046 39(18), 7046–7054, doi:10.1021/es050400s, 2005b.

1047 Raschka, S.: Python machine learning, edited by A. Hussain, Packt Publishin Ltd., Birmingham,  
1048 UK. [online] Available from: www.packtpub.com, 2016.

1049 [Rindelaub, J. D., Borca, C. H., Hostetler, M. A., Slade, J. H., Lipton, M. A., Slipchenko, L. V.,  
1050 and Shepson, P. B.: The acid-catalyzed hydrolysis of an  \$\alpha\$ -pinene-derived organic nitrate:  
1051 kinetics, products, reaction mechanisms, and atmospheric impact, Atmos. Chem. Phys., 16,  
1052 15425-15432, 10.5194/acp-16-15425-2016, 2016.](#)

1053 Rindelaub, J. D., Mcavey, K. M., and Shepson, P. B.: The photochemical production of organic  
1054 nitrates from  $\alpha$ -pinene and loss via acid-dependent particle phase hydrolysis, Atmos. Environ.,  
1055 100, 193–201, doi:10.1016/j.atmosenv.2014.11.010, 2015.

1056 Rindelaub, J. D., McAvey, K. M., and Shepson, P. B.: Determination of  $\alpha$ -pinene-derived organic  
1057 nitrate yields: Particle phase partitioning and hydrolysis, Atmos. Chem. Phys. Discussions., 2014.

1058 Roberts, J. M.: Chemistry of organic nitrates, Atmos. Environ., 24(2), 243–287

1059 Rollins, A. W., Browne, E. C., Pusede, S. E., Wooldridge, P. J., Gentner, D. R., Goldstein, A. H.,  
1060 Liu, S., Day, D. A., and Cohen, R. C.: Evidence for NO<sub>x</sub> control over nighttime SOA formation,  
1061 Science, 267(September), 1210–1212

1062 Rollins, A. W., Pusede, S., Wooldridge, P., Min, K.-E., Gentner, D. R., Goldstein, A. H., Liu,  
1063 S., Day, D. A., Russell, L. M., Rubitschun, C. L., Surratt, J. D., and Cohen, R. C.: Gas/particle  
1064 partitioning of total alkyl nitrates observed with TD-LIF in Bakersfield, J. Geophys. Res. Atmos.,  
1065 118(12), 6651–6662, doi:10.1002/jgrd.50522, 2013.

1066 Rousseeuw, P. J.: Silhouettes: A graphical aid to the interpretation and validation of cluster  
1067 analysis, J. Comput. Appl. Math., 20(C), 53–65, doi:10.1016/0377-0427(87)90125-7, 1987.

1068 Saunders, S. M., Jenkin, M. E., Derwent, R. G., and Pilling, M. J.: Protocol for the development  
1069 of the Master Chemical Mechanism, MCM v3 (Part A): Tropospheric degradation of non-  
1070 aromatic volatile organic compounds, Atmos. Chem. Phys., 3(1), 161–180, doi:10.5194/acp-3-  
1071 161-2003, 2003.

1072 Singh, H. B. and Hanst, P. L.: Peroxyacetyl nitrate (PAN) in the unpolluted atmosphere: An  
1073 important reservoir for nitrogen oxides, Geophys. Res. Lett., 8(8), 941–944

1074 Smith, J. N., Dunn, M. J., VanReken, T. M., Iida, K., Stolzenburg, M. R., McMurry, P. H., and  
1075 Huey, L. G.: Chemical composition of atmospheric nanoparticles formed from nucleation in  
1076 Tecamac, Mexico: Evidence for an important role for organic species in nanoparticle growth,  
1077 Geophys. Res. Lett., 35(4), 2–6, doi:10.1029/2007GL032523, 2008.

Deleted: -----Page Break-----  
¶

1080 Spittler, M., Barnes, I., Bejan, I., Brockmann, K. J. J., Benter, T., and Wirtz, K.: Reactions of  
1081 NO<sub>3</sub> radicals with limonene and  $\alpha$ -pinene: Product and SOA formation, *Atmos. Environ.*, 40(3),  
1082 116–127, doi:10.1016/j.atmosenv.2005.09.093, 2006.

1083 [Stark, H., Yatavelli, R. L. N., Thompson, S. L., Kang, H., Krechmer, J. E., Kimmel, J. R., Palm,](#)  
1084 [B. B., Hum, W., Hayes, P. L., Day, D. A., Campuzano-Jost, P., Canagaratna, M. R., Jayne, J. T.,](#)  
1085 [Worsnop, D. R., and Jiminez, J. L.: Impact of thermal decomposition on thermal desorption](#)  
1086 [instruments: Advantage of hermogram analysis for quantifying volatility distributions of organic](#)  
1087 [species, \*Environ. Sci. Technol.\*, 51, 15, 85491-8500, 2017.](#)

1088 Sun, T., Wang, Y., Zhang, C., Sun, X., and Wang, W.: The chemical mechanism of the limonene  
1089 ozonolysis reaction in the SOA formation: A quantum chemistry and direct dynamic study,  
1090 *Atmos. Environ.*, 45(9), 1725–1731, doi:10.1016/j.atmosenv.2010.12.054, 2011.

1091 Temple, P. J. and Taylor, O. C.: World-wide ambient measurements of peroxyacetyl nitrate  
1092 (PAN) and implications for plant injury, *Atmos. Environ.*, 17(8), 1583–1587, doi:10.1016/0004-  
1093 6981(83)90311-6, 1983.

1094 Tolocka, M. P., Jang, M., Ginter, J. M., Cox, F. J., Kamens, R. M., and Johnston, M. V.:  
1095 Formation of oligomers in secondary organic aerosol, *Environ. Sci. Technol.*, 38(5), 1428–1434,  
1096 doi:10.1021/es035030r, 2004.

1097 Wainman, T., Zhang, J., Weschler, C. J., and Lioy, P. J.: Ozone and limonene in indoor air: A  
1098 source of submicron particle exposure, *Environ. Health Perspect.*, 108(12), 1139–1145,  
1099 doi:10.1289/ehp.001081139, 2000.

1100 Van Der Walt, S., Colbert, S. C., and Varoquaux, G.: The NumPy array: A structure for efficient  
1101 numerical computation, *Comput. Sci. Eng.*, 13(2), 22–30, doi:10.1109/MCSE.2011.37, 2011.

1102 Wehner, B., Petäjä, T., Boy, M., Engler, C., Birmili, W., Tuch, T., Wiedensohler, A., and  
1103 Kulmala, M.: The contribution of sulfuric acid and non-volatile compounds on the growth of  
1104 freshly formed particles at Melpitz, *Geophys. Res. Lett.*, 32(L17810), doi:10.1063/1.4803246,  
1105 2005.

1106 [Xu, L., Williams, L. R., Young, D. E., Allan, J. D., Coe, H., Massoli, P., Fortner, E., Chhabra, P.,](#)  
1107 [Herndon, S., Brooks, W. A., Jayne, J. T., Worsnop, D. R., Aiken, A. C., Liu, S., Gorkowski, K.,](#)  
1108 [Dubey, M. K., Fleming, Z. L., Visser, S., Prévôt, A. S. H., and Ng, N. L.: Wintertime aerosol](#)  
1109 [chemical composition, volatility, and spatial variability in the greater London area, \*Atmos. Chem.\*](#)  
1110 [Phys., 16, 1139–1160, doi:10.5194/acp-16-1139-2016, 2016.](#)

1111 Yatavelli, R. L. N., Lopez-Hilfiker, F., Wargo, J. D., Kimmel, J. R., Cubison, M. J., Bertram, T.  
1112 H., Jimenez, J. L., Gonin, M., Worsnop, D. R., and Thornton, J. A.: A Chemical Ionization High-  
1113 Resolution Time-of-Flight Mass Spectrometer Coupled to a Micro Orifice Volatilization  
1114 Impactor (MOVI-HRToF-CIMS) for analysis of gas and particle-phase organic species, *Aerosol*  
1115 *Sci. Technol.*, 46(12), 1313–1327, doi:10.1080/02786826.2012.712236, 2012.

1116 Youssefi, S. and Waring, M. S.: Transient secondary organic aerosol formation from d-limonene  
1117 and  $\alpha$ -pinene ozonolysis in indoor environments, *Indoor Air 2014 - 13th Int. Conf. Indoor Air*  
1118 *Qual. Clim.*, 145–152 [online] Available from: [Deleted: -----Page Break-----  
¶](http://www.scopus.com/inward/record.url?eid=2-</a></p></div><div data-bbox=)

Moved up [5]: P. L.

Moved up [1]: L.,

Deleted: Tuazon, E. C., Carter, W.

Deleted: and Atkinson, R.: Thermal decomposition of peroxyacetyl nitrate and reactions of acetyl peroxy radicals with NO and NO<sub>2</sub> over the temperature range 283–313 K, *J. Phys. Chem.*, 95, 2434–2437 ¶

Deleted: Wooldridge, P. J., Perring, A.

Moved up [7]: E.,

Deleted: Bertram, T

Moved up [8]: . H.,

Deleted: Flocke, F.

Moved up [4]: M.,

Deleted: Roberts, J.

Moved up [9]: M.,

Moved up [6]: A.,

Deleted: Singh, H. B., Huey, L. G

Moved up [13]: ., Thornton, J. A.,

Deleted: Wolfe, G.

Moved up [11]: M.,

Moved up [12]: L.,

Deleted: Murphy, J. G., Fry, J.

Deleted: Rollins, A. W., Lafranchi, B. W., and Cohen, R. C.: Total Peroxy Nitrates (EPNs) in the atmosphere: The Thermal Dissociation-Laser Induced Fluorescence (TD-LIF) technique and comparisons to speciated PAN measurements, *Atmos. Meas. Tech.*, 3(3), 593–607, doi:10.5194/amt-3-593-2010, 2010. ¶

1152 s2.0-84924705682&partnerID=tZOtx3y1, 2014.

1153 Zhang, J., Hartz, K. E. H., Pathak, R. K., Pandis, S. N., and Donahue, N. M.: Secondary organic  
1154 aerosol formation from limonene ozonolysis: NO<sub>x</sub> and ultraviolet effects, *J. Phys. Chem. A*,  
1155 110(38), 11053–11063

1156 Ziemann, P. J. and Atkinson, R.: Kinetics, products, and mechanisms of secondary organic  
1157 aerosol formation, *Chem. Soc. Rev.*, 41(19), 6582, doi:10.1039/c2cs35122f, 2012.

1158

Page 6: [1] Deleted		Author		
---------------------	--	--------	--	--

1	160	15	10.7	8.1
2	95	40	2.4	8

Page 6: [2] Deleted		Author		
---------------------	--	--------	--	--

11	850	95	8.9	25
12	850	150	5.7	47

---